ELSEVIER

Neurobiology of Aging 31 (2010) 1401–1418

NEUROBIOLOGY OF AGING

www.elsevier.com/locate/neuaging

Longitudinal MRI atrophy biomarkers: Relationship to conversion in the ADNI cohort

Shannon L. Risacher[a,b], Li Shen[a,b,d], John D. West[a,c], Sungeun Kim[a,d], Brenna C. McDonald[a,c], Laurel A. Beckett[e], Danielle J. Harvey[e], Clifford R. Jack, Jr.[f], Michael W. Weiner[g,h], Andrew J. Saykin[a,b,c,*], and the Alzheimer's Disease Neuroimaging Initiative (ADNI)

[a] *Center for Neuroimaging, Department of Radiology and Imaging Sciences, Indianapolis, IN, United States*
[b] *Medical Neuroscience Program, Stark Neurosciences Research Institute, Indianapolis, IN, United States*
[c] *Indiana Alzheimer Disease Center, Indianapolis, IN, United States*
[d] *Center for Computational Biology and Bioinformatics, Indiana University School of Medicine, Indianapolis, IN, United States*
[e] *Division of Biostatistics, School of Medicine, University of California, Davis, Davis, CA, United States*
[f] *Mayo Clinic, Rochester, MN, United States*
[g] *Departments of Radiology, Medicine, and Psychiatry, University of California, San Francisco, San Francisco, CA, United States*
[h] *Department of Veterans Affairs Medical Center, San Francisco, CA, United States*

Received 16 February 2010; Received in revised form 25 April 2010; accepted 27 April 2010

Abstract

Atrophic changes in early Alzheimer's disease (AD) and amnestic mild cognitive impairment (MCI) have been proposed as biomarkers for detection and monitoring. We analyzed magnetic resonance imaging (MRI) atrophy rate from baseline to 1 year in 4 groups of participants from the Alzheimer's Disease Neuroimaging Initiative (ADNI): AD ($n = 152$), converters from MCI to probable AD (MCI-C, $n = 60$), stable MCI (MCI-S, $n = 261$), and healthy controls (HC, $n = 200$). Scans were analyzed using multiple methods, including voxel-based morphometry (VBM), regions of interest (ROIs), and automated parcellation, permitting comparison of annual percent change (APC) in neurodegeneration markers. Effect sizes and the sample required to detect 25% reduction in atrophy rates were calculated. The influence of *APOE* genotype on APC was also evaluated. AD patients and converters from MCI to probable AD demonstrated high atrophy APCs across regions compared with minimal change in healthy controls. Stable MCI subjects showed intermediate atrophy rates. *APOE* genotype was associated with APC in key regions. In sum, APC rates are influenced by *APOE* genotype, imminent MCI to AD conversion, and AD-related neurodegeneration.

Keywords: Alzheimer's Disease Neuroimaging Initiative (ADNI); Magnetic resonance imaging (MRI); Voxel-based morphometry (VBM); Mild cognitive impairment (MCI); Hippocampus; Longitudinal change; Genetic factors; Apolipoprotein E (APOE) epsilon 4 allele

1. Introduction

Alzheimer's disease (AD) is the most common age-related neurodegenerative disease affecting nearly 25 million people worldwide, a number expected to triple in the next 50 years (Ferri et al., 2005; Wimo et al., 2003). Patients with AD show significant impairment in multiple cognitive domains, including deficits in memory and executive functioning. Progress in the early clinical diagnosis of AD has led to the characterization of a prodromal syndrome featuring relatively isolated memory deficits termed "amnestic mild cognitive impairment" (mild cognitive impairment; MCI) (Petersen and Negash, 2008; Petersen et al., 2001). Amnestic MCI is conceptualized as a preliminary stage of AD-associated neurodegeneration with the majority of pa-

* Corresponding author at: IU Center for Neuroimaging, Department of Radiology and Imaging Sciences, Indiana University, School of Medicine, 950 W Walnut St., R2 E124, Indianapolis, IN 46202, United States. Tel.: +1 317 278 6947; fax: +1 317 274 1067.
E-mail address: asaykin@iupui.edu (A.J. Saykin).

0197-4580/$ – see front matter © 2010 Elsevier Inc. All rights reserved.
doi:10.1016/j.neurobiolaging.2010.04.029

tients eventually progressing to AD at a rate of 10%–15% per year (Petersen et al., 1999; Petersen, 2000).

The increasing recognition that early diagnosis and therapeutic intervention will be necessary to prevent the development of AD underscores the need to develop sensitive and specific biomarkers for detecting and monitoring MCI and AD. Structural magnetic resonance imaging (MRI) has shown significant promise as a biomarker to detect early MCI and AD-associated changes, as well as to predict the rate of disease progression (de Leon et al., 2007; Jack et al., 1999; Risacher and Saykin, in press). Cross-sectional studies evaluating the utility of structural MRI in detecting neurodegeneration have identified significant brain atrophy in patients with MCI and AD, particularly in regions of the medial temporal lobe (MTL) using regional volumetric extraction tools such as manual tracing of regions of interest (ROIs) (de Leon et al., 2007; De Toledo-Morrell et al., 2000; Dickerson et al., 2001; Du et al., 2001; Jack et al., 1992; Killiany et al., 2002; Pennanen et al., 2004; Saykin et al., 2006; Xu et al., 2000), and more recently, automated segmentation and parcellation of target regions (Becker et al., 2006; Colliot et al., 2008; Du et al., 2007; Fischl and Dale, 2000a; Risacher et al., 2009). Other semiautomated tools which provide 3-dimensional mapping of brain morphology, including voxel-based morphometry (VBM), tensor-based morphometry (TBM) and related techniques have also identified significant global and local tissue changes in patients with MCI and AD, including decreased whole brain, hippocampal, and temporal lobar gray matter (GM) density (Busatto et al., 2003; Chetelat et al., 2002; Frisoni et al., 2002; Jack et al., 2008b; Karas et al., 2003; Pennanen et al., 2005; Saykin et al., 2006; Trivedi et al., 2006). Structural MRI techniques have also been shown to provide sensitive prediction of disease progression. Hippocampal volume and GM density, as well as measures of MTL volume and cortical thickness, have been identified as sensitive biomarkers for predicting conversion from MCI to probable AD (Apostolova et al., 2006; Bozzali et al., 2006; Chetelat et al., 2005; Devanand et al., 2007; Jack et al., 1999; Kinkingnehun et al., 2008; Risacher et al., 2009; Visser et al., 2002; Whitwell et al., 2008b).

Longitudinal monitoring of rate of decline on MRI measures has also proven sensitive to AD-related changes. Increased rates of whole brain and MTL atrophy in patients with MCI and AD relative to healthy elderly controls (HC) are routinely reported in studies of brain aging and dementia (for recent review, see Frisoni et al., 2010). Manual tracing or automated ROI techniques and analysis of deformation fields reflecting brain shrinkage are the most commonly employed methods for evaluating longitudinal changes in global and regional volume, particularly in the MTL. Previous studies have reported rates of hippocampal annual decline of 4.5% in patients with AD and 3% in patients with MCI in contrast to 1% decline in controls (for meta-analysis see Barnes et al., 2009). Furthermore, increased atrophy rates can also predict future decline, including MCI to probable AD conversion (Erten-Lyons et al., 2006; Jack et al., 2000, 2004, 2005; Sluimer et al., 2008; Stoub et al., 2008), with patients who convert from MCI to probable AD showing higher rates of hippocampal atrophy compared with patients with a stable diagnosis of MCI, reported as 3.5% and 2.2%, respectively (Jack et al., 2000, 2004).

Genetic factors play a significant role in the development and progression of MCI and AD. Genetic variation in the apolipoprotein E gene (*APOE*) is the most commonly reported genetic risk factor associated with AD, with the presence of a single $\varepsilon 4$ allele conferring a 2-fold or 3-fold increased risk of developing AD and 2 $\varepsilon 4$ alleles associated with nearly an 11-fold increased risk (Bertram and Tanzi, 2008; Farrer et al., 1997; Gatz et al., 2006). In addition to an increased risk of AD, the presence of an $\varepsilon 4$ allele has been associated with imaging markers. An increased rate of hippocampal and whole brain atrophy in $\varepsilon 4$ carriers has been reported in nondemented individuals, as well as in MCI and AD patients, in some studies (Cohen et al., 2001; Fjell et al., 2010a; Fleisher et al., 2005; Hamalainen et al., 2008; Jack et al., 2008c, 2008d; Mori et al., 2002; Morra et al., 2009; Schuff et al., 2009; Wang et al., 2006) but not in others (Du et al., 2006; Wang et al., 2009).

The Alzheimer's Disease Neuroimaging Initiative (ADNI) is a 5-year consortium study designed to assess the utility of various biomarkers for detecting early changes associated with MCI and AD and predicting disease course over time, including cross-sectional and longitudinal neuroimaging biomarkers from structural MRI and positron emission tomography (PET), genetic factors, psychometric scores, cerebrospinal fluid (CSF) markers, and other variables. A number of studies utilizing MRI data from this cohort have been published within the last year. Using both ROI and 3-dimensional mapping techniques the expected differences in structural MRI markers have been found between diagnostic (AD, MCI, HC) groups at baseline assessment, including atrophy in hippocampal and other MTL regions and enlarged ventricles in patients with AD and MCI (Chou et al., 2009; Chupin et al., 2009; Fan et al., 2008; Fennema-Notestine et al., 2009; Nestor et al., 2008; Querbes et al., 2009; Risacher et al., 2009; Vemuri et al., 2009; Walhovd et al., 2008). Hippocampal volume has also been found to be sensitive and specific for predicting 1-year conversation from MCI to probable AD (Calvini et al., 2009; Chupin et al., 2009; McEvoy et al., 2009; Misra et al., 2009; Nestor et al., 2008; Querbes et al., 2009; Risacher et al., 2009). MRI studies of the ADNI cohort have also examined longitudinal change in brain volumes using ROI and whole-brain structural change techniques (e.g., Jacobian determinants, boundary shift integral [BSI]), and have detected differences in annual change in whole brain volume, hippocampal volume, and ventricular volume as a function of baseline diagnostic group (AD, MCI, HC) (Evans et al., 2009; Fjell et al., 2010b; Ho et al., 2009;

Holland et al., 2009; Hua et al., 2009; Jack et al., 2009; Leow et al., 2009; McDonald et al., 2009; McEvoy et al., 2009; Misra et al., 2009; Morra et al., 2009; Nestor et al., 2008; Schuff et al., 2009) and of *APOE* ε4 genotype (Fjell et al., 2010a; Morra et al., 2009; Nestor et al., 2008; Schuff et al., 2009). Several studies have reported larger declines in whole brain and regional volumes, as well as larger ventricular volume increases in MCI to AD converters than MCI nonconverters (Evans et al., 2009; Leow et al., 2009; Misra et al., 2009; Nestor et al., 2008).

In order to better evaluate the effectiveness of future disease modifying therapeutics, biomarkers of disease state and progression are likely to be more sensitive and reliable than clinical measures, which may be highly variable within and between participants. When designing clinical trials, an important consideration is the sample size needed to detect a therapeutic effect that is both statistically significant and clinically meaningful in a target biomarker with 80% or 90% power. Several previous studies in the ADNI cohort have calculated the relative sample size needed to detect a hypothetical treatment-induced 25% reduction in brain atrophy for various regional MRI markers and have suggested that to achieve 80% power approximately 35–100 AD and 100–200 MCI participants are required (Ho et al., 2009; Holland et al., 2009; Hua et al., 2009; Nestor et al., 2008).

Despite the extensive MRI analyses in AD and MCI, prior studies have not directly compared the relative sensitivity of longitudinal changes in GM density and volume, cortical thickness and ROI volumes in relation to changes in clinical status. In ADNI, longitudinal studies have primarily focused on baseline diagnostic groups rather than 1-year clinical conversion status. The present study was designed to compare the annual percent change (APC) of different types of structural MRI markers in groups defined by baseline diagnosis and 1-year MCI to AD conversion status using the final 1-year sample. We hypothesized that patients with more advanced clinical indicators of disease progression, particularly AD and converters from MCI to probable AD (MCI-C), would show significantly greater APC in major structural MRI markers. We also evaluated the relative sensitivity of these markers to progression of atrophy over time. Because of the important implications for design of future therapeutic trials of disease-modifying agents, we also calculated the sample size needed to detect a 25% reduction in atrophy rate for selected markers. We hypothesized that the MTL changes would constitute the most sensitive regional markers of progression and therefore require the smallest potential sample sizes. Prior ADNI reports have not evaluated the sample size needed for trials in rapidly progressing MCI participants (MCI converters; MCI-C) compared with stable MCI participants (MCI-S), an important distinction for trial design. Additionally, previous reports have focused primarily on sample sizes needed for MRI markers that were extracted using a single technique. In the present study, we compared GM density and volume, cortical thickness, and ROI volumetric markers. Finally, we assessed the impact of *APOE* genotype on APC in several key target regions, which to date has not been examined in patients who converted from MCI to probable AD in the ADNI cohort to our knowledge. We hypothesized that the presence of an ε4 allele would increase the annual rate of decline in selected MRI markers of MTL integrity.

2. Methods

2.1. ADNI

ADNI is a consortium study initiated in 2004 by the National Institute on Aging (NIA), the National Institute of Biomedical Imaging and Bioengineering (NIBIB), the Food and Drug Administration (FDA), private pharmaceutical companies, and nonprofit organizations. More than 800 participants age 55–90 have been recruited from 59 sites across the USA and Canada to be followed for 2–3 years, with repeated structural MRI and positron emission tomography scans and functional, psychological, and psychometric test data collected every 6 or 12 months. For additional information about ADNI, see www.adni-info.org and Mueller et al. (2005a, 2005b).

2.2. MRI scans

Raw baseline 1.5 T MRI scans from 820 participants were downloaded from the ADNI public web site (www.loni.ucla.edu/ADNI/) onto local servers at Indiana University School of Medicine between January and April 2008 and processed using Freesurfer (version 4, http://surfer.nmr.mgh.harvard.edu/, Boston, MA) and VBM as implemented in SPM5 (www.fil.ion.ucl.ac.uk/spm/, London, UK) as previously described (Risacher et al., 2009). All available 1.5 T magnetization-prepared rapid gradient-echo (MP-RAGE) scans collected at the 1-year follow-up visit ("12-month scans") were also downloaded for all participants ($n = 693$) as of June 2009. A minimum of 2 MP-RAGE images were acquired at each time point for each participant, using a standard MP-RAGE protocol that was selected and tested by ADNI (Jack et al., 2008a).

Participants were only included in the present analysis if their baseline and 12-month MRI scans were successfully preprocessed. Four participants failed Freesurfer processing and were not included in any analyses. Thirty additional participants were excluded from only the VBM analyses due to failed processing of scans from either the baseline or 12-month visit. Participants who did not have either baseline ($n = 2$) or 12-month ($n = 124$) scans were also excluded. Included participants ($n = 673$ for Freesurfer analyses, $n = 643$ for VBM analyses) were divided into groups by baseline and 1-year clinical diagnosis and 12-month MCI to probable AD conversion status, resulting in 4 groups: (1) participants with a stable AD diagnosis (AD; $n = 152$ for Freesurfer analyses, $n = 143$ for VBM analy-

ses); (2) participants with an MCI diagnosis at baseline who converted to a diagnosis of probable AD at either the 6- or 12-month time point (MCI-C; $n = 60$ for Freesurfer analyses, $n = 57$ for VBM analyses); (3) participants with a stable diagnosis of MCI (MCI-S; $n = 261$ for Freesurfer analyses, $n = 253$ for VBM analyses); and (4) participants with a stable designation of healthy elderly control (HC; $n = 200$ for Freesurfer analyses, $n = 190$ for VBM analyses). Participants who showed other forms of conversion, reversion, or otherwise unstable diagnostic designation were excluded (e.g., conversion from HC to MCI at the 6-month visit, followed by a reversion from MCI to HC at the 12-month visit, etc.; $n = 16$). Details of the ADNI design, participant recruitment, clinical testing, and additional methods have been published previously (Jack et al., 2008; Mueller et al., 2005a, 2005b; Petersen et al., 2010) and at www.adni-info.org.

2.3. Demographic and clinical data

Demographic information, *APOE* genotype, neuropsychological test scores, and diagnosis information for all analyzed visits were downloaded from the ADNI clinical data repository (https://www.loni.ucla.edu/ADNI/Data/ADCS_Download.jsp). The "8/9/09" version of the ADNI clinical database was used for all analyses. By this time all 1-year clinical and scan data were complete. Participants were classified into groups based on baseline and 12-month diagnoses as reported in the conversion/reversion database.

To evaluate the impact of *APOE* genotype on annual rate of atrophy, we also classified participants by the presence or absence of an *APOE* ε4 allele. Given the unknown impact of having an ε2ε4 genotype (i.e., possessing a potential protective allele [ε2] and a risk allele [ε4] for AD), we chose to run analyses both including and excluding the ε2ε4 participants ($n = 13$; 3 AD, 7 MCI-S, 3 HC). We found similar results from the 2 comparisons (data not shown), and thus, chose to use the largest available sample in the results presented in this report. For the evaluation of hippocampal volume and entorhinal cortex (EC) thickness, 673 participants were included: 99 AD, 35 MCI-C, 143 MCI-S, and 56 HC who were *APOE* ε4 positive (ε2ε4, ε3ε4, or ε4ε4 genotypes) and 53 AD, 25 MCI-C, 118 MCI-S, and 144 HC who were *APOE* ε4 negative (ε2ε2, ε2ε3, or ε3ε3 genotypes). Thirty participants were excluded due to failed VBM processing, as previously described. Thus, the analysis of the effect of *APOE* ε4 genotype on bilateral mean hippocampal GM density and volume included the following participants ($n = 643$): 95 AD, 34 MCI-C, 142 MCI-S, and 53 HC who were *APOE* ε4 positive and 48 AD, 23 MCI-C, 111 MCI-S, and 137 HC who were *APOE* ε4 negative.

2.4. Image processing

2.4.1. VBM

Scans were processed with VBM in SPM5, using previously described methods (Ashburner and Friston, 2000; Good et al., 2001; Mechelli et al., 2005). Briefly, after conversion from DICOM to NIfTI, both baseline MP-RAGE scans were aligned to the T1 template and both 12-month scans were coregistered to the T1-aligned baseline scans. After alignment, all scans were bias corrected and segmented into GM, white matter (WM), and CSF compartments using standard SPM5 templates. GM maps were normalized to Montreal Neurological Institute (MNI) atlas space as 1mm × 1mm × 1 mm voxels and smoothed using a 10 mm full-width at half maximum (FWHM) Gaussian kernel. Both modulated and unmodulated GM maps were generated. To maximize signal and minimize variability in the imaging markers, we chose to create a mean GM image of the 2 independent MP-RAGE-derived GM maps using SPM5. These mean GM volumes were then employed in all subsequent VBM analyses. This process was completed for both unmodulated and modulated normalized GM maps from each individual, yielding a mean GM density image and a mean GM volume image, respectively.

2.4.2. Regions of Interest (ROIs)

A hippocampal ROI template was created by manual tracing of the left and right hippocampi in an independent sample of 40 HC participants enrolled in a study of brain aging and MCI (McHugh et al., 2007; Saykin et al., 2006; Shen et al., 2010). Hippocampal GM density and GM volume values were extracted from baseline and 12-month mean GM maps from VBM as previously described (Risacher et al., 2009). Additionally, mean GM density and mean GM volume were extracted from 90 cortical and 26 cerebellar regions using MarsBaR ROI templates (http://marsbar.sourceforge.net/; Brett et al., 2002). Mean lobar measures from MarsBaR regions were calculated from target ROIs as follows: mean frontal lobe is the mean of GM values from inferior frontal operculum and triangularis, inferior, medial, middle, and superior orbital frontal, middle and superior frontal, and medial superior frontal regions; mean parietal lobe is the mean of inferior and superior parietal, angular gyrus, supramarginal gyrus, and precuneus GM values; and mean temporal lobe value is the mean of GM values from the amygdala and hippocampus, middle and superior temporal pole, inferior, middle, and superior temporal gyri, and fusiform, Heschl's, lingual, olfactory, and parahippocampal gyri.

2.4.3. Automated parcellation

Bilateral volumetric and cortical thickness estimates from the baseline and 12-month scans were extracted using Freesurfer V4 (Dale et al., 1999; Fischl and Dale, 2000b; Fischl et al., 1999, 2002; Shen et al., 2010) as previously described (Risacher et al., 2009). Each scan from each time point was processed independently. The final extracted values were then used to calculate a mean volume or cortical thickness for each region for both the baseline and 12-month time points. Mean lobar cortical thickness measures were calculated from selected ROI mean cortical thick-

nesses from Freesurfer as follows: mean frontal lobe was the mean of caudal midfrontal, rostral midfrontal, lateral orbitofrontal, medial orbitofrontal, and superior frontal gyri, pars opercularis, oribitalis, and triangularis, and frontal pole thicknesses; mean parietal lobe was the mean of inferior parietal, superior parietal, supramarginal gyri, and precuneus thicknesses; and mean temporal lobe was the mean of the fusiform, lingual, parahippocampal, inferior temporal, middle temporal, and lateral temporal gyri, as well as temporal and transverse temporal pole thicknesses.

2.5. VBM statistical analysis

A two-way analysis of variance (ANOVA) assessing time and group membership (AD, MCI-C, MCI-S, HC) was performed to compare the change over 1 year between groups using the smoothed, unmodulated, normalized mean GM maps. Statistical analyses were performed on a voxel-by-voxel basis using a general linear model (GLM) approach implemented in SPM5. A threshold of $p < 0.0001$ (uncorrected for multiple comparisons) and minimum cluster size (k) of 27 voxels was considered significant. We chose to show the VBM comparison images at this threshold ($p < 0.0001$ uncorrected) for display purposes although all comparisons, except for AD versus MCI-C, survive $p < 0.05$ with a false discovery rate (FDR) correction for multiple comparisons and all 6 comparisons have at least 1 cluster which survives $p < 0.01$ with a family-wise error (FWE) multiple comparison correction. Baseline age, gender, years of education, handedness, and baseline mean intracranial volume (ICV) were included as covariates, and an explicit GM mask was used to restrict analyses to GM regions.

2.6. Other statistical analyses

Annual percent change (APC) estimates were calculated using mean values from left and right ROIs from baseline and 12-month scans for each participant using the following equation.

$$\mathrm{APC} = \frac{\dfrac{(\text{12-mo ROI value} - \text{BL ROI value})}{(\text{BL ROI value})}}{(\text{time [years] between BL and 12-mo visits})}$$

A one-way multivariate ANOVA was used to assess differences in mean MRI change measures between groups. Baseline age, gender, education, handedness, and baseline mean ICV were included as covariates. Pairwise comparisons with a Bonferroni adjustment for multiple comparisons were also used to assess differences between individual group pairs. One-way ANOVA and χ^2 tests were used to determine group differences in demographic variables, as well as baseline values and annual change of psychometric test scores. SPSS (version 17.0.2, Chicago, IL) was used for statistical analysis.

The sample size needed to detect a 25% reduction in mean APC (2-sided t test; $\alpha = 0.05$) with 80% or 90% power was also calculated using Microsoft Excel (2007) for the absolute change over 1 year of all target variables for all 4 diagnostic groups to determine the relative sensitivity of MRI change measures for monitoring atrophy progression. Only participants with values for all analyzed regions were included in these calculations ($n = 643$; 143 AD, 57 MCI-C, 253 MCI-S, 190 HC). Sample size was calculated using the following equation:

$$n = \frac{2\sigma^2(Z_{1-\alpha/2} + Z_{\text{power}})^2}{(0.25\beta)^2}$$

where n is the target sample size, $\alpha = 0.05$, β is the adjusted mean absolute change, σ is the standard deviation of the measure, and z_a is the value from the standard distribution for 80% or 90% power (Ho et al., 2009; Hua et al., 2009; Rosner, 1990).

Effect sizes for the comparisons between pairs of diagnostic groups were also calculated for bilateral mean APC and baseline values of selected imaging markers. Left and right adjusted means, covaried for baseline age, gender, education, handedness, and baseline mean ICV, were averaged to yield a bilateral estimate. These bilateral mean values were then used to calculate the effect size (Cohen's d) between group pairs for all imaging measures in Microsoft Excel (2007) as follows:

$$d = \frac{(\mathrm{M}_1 - \mathrm{M}_2)}{\sqrt{\left[\left(\sigma_1^2 + \sigma_2^2\right)/2\right]}}$$

where, for a target marker, M_1 = mean value for group 1, M_2 = mean value for group 2, σ_1 = standard deviation for group 1, and σ_2 = standard deviation for group 2 (Cohen, 1988). In order to accurately compare the resulting effect sizes, only participants with values for all analyzed regions were included in this comparison ($n = 643$; 143 AD, 57 MCI-C, 253 MCI-S, 190 HC).

Finally, a two-way ANOVA was used to assess the impact of diagnostic group and *APOE* ε4 genotype on sensitive imaging phenotypes as determined by large effect sizes in the comparison of MCI-C and MCI-S participants, namely the APC in bilateral mean hippocampal GM density and volume, hippocampal volume, and EC thickness. Additionally, two-sample t tests were used to evaluate the influence of *APOE* ε4 genotype within each of the 4 diagnostic groups on MTL change measures. Age, gender, education, handedness, and baseline ICV were included as covariates in all analyses. All graphs were created using SigmaPlot (version 10.0, San Jose, CA).

3. Results

3.1. Group characteristics and change in psychometric scores

Demographic information and the baseline values and change in selected psychometric scores over the first year are found in Table 1. Significant differences were demon-

Table 1
Demographic information and neuropsychological test scores

	AD (n = 152)	MCI-C (n = 60)	MCI-S (n = 261)	HC (n = 200)	p-value	Significant pair comparisons ($p < 0.05$)
Baseline age	75.33 (0.5)	74.04 (0.9)	75.07 (0.4)	75.95 (0.5)	NS	None
12-month age	76.41 (0.5)	75.11 (0.9)	76.15 (0.4)	77.04 (0.5)	NS	None
Education	14.82 (0.2)	15.15 (0.4)	15.89 (0.2)	16.08 (0.2)	$p < 0.001$	HC, MCI-S > AD
Gender (M, F)	80, 72	35, 25	166, 95	105, 95	$p = 0.06$	MCI-S versus AD, HC
Handedness (R, L)	144, 8	55, 5	239, 22	185, 15	NS	None
ApoE genotype (% ApoE4+)	65.13%	58.33%	54.79%	28.00%	$p < 0.001$	AD, MCI-C, MCI-S > HC
Baseline CDR-SB	4.18 (0.1)	2.00 (0.1)	1.52 (0.1)	0.02 (0.1)	$p < 0.001$	AD > MCI-C > MCI-S > HC
12-month change in CDR-SoB[a]	+2.13 (0.1)	+2.64 (0.2)	+1.26 (0.1)	+1.1 (0.1)	$p < 0.001$	AD, MCI-C > MCI-S, HC
Baseline MMSE	23.53 (0.1)	26.58 (0.2)	27.11 (0.1)	29.11 (0.1)	$p < 0.001$	HC > MCI-S, MCI-C >AD
12-month change in MMSE[b]	−1.88 (0.7)	−2.56 (0.4)	−0.35 (0.2)	0.00 (0.2)	$p < 0.001$	HC, MCI-S > MCI-C, AD
Baseline RAVLT[c]	23.25 (0.7)	26.20 (1.1)	32.00 (0.5)	43.65 (0.6)	$p < 0.001$	HC > MCI-S > MCI-C, AD
12-month change in RAVLT[d]	−2.91 (0.5)	−2.68 (0.8)	−0.81 (0.4)	+0.3 (0.5)	$p < 0.001$	HC > MCI-C, AD; MCI-S > AD
Baseline ICV	1552677.32 (13807.5)	1566297.83 (21976.7)	1570616.06 (10537.0)	1534944.90 (12037.1)	NS	None

Data are given as mean (standard error of the mean) or n.
Key: AD, Alzheimer's disease; CDR-SB, Clinical Dementia Rating-Sum of Boxes; F, female; HC, healthy control; ICV, intracranial volume; L, left; M, male; MCI-C, converters from mild cognitive impairment to probable AD; MCI-S, mild cognitive impairment-stable; MMSE, Mini Mental State Examination; NS, nonsignificant; R, right, RAVLT, Rey Auditory Verbal Learning Test.
[a] Seven participants missing data (2 AD, 1 MCI-S, 4 HC).
[b] Two participants missing data (1 MCI-S, 1 HC).
[c] Three participants missing data (1 AD, 2 HC).
[d] Fourteen participants missing data (8 AD, 3 MCI-S, 3 HC).

strated in education level ($F = 6.53$, $p < 0.001$) and *APOE* genotype (percentage positive for at least 1 $\varepsilon 4$ allele; $\chi^2 = 56.64$, $p < 0.001$), specifically between HCs and patient groups. Expected differences between groups in psychometric test scores were found to be significant for both baseline scores and annual change in scores on the Clinical Dementia Rating-Sum of Boxes (CDR-SB; baseline, $F = 532.91$, $p < 0.001$; annual change, $F = 21.42$, $p < 0.001$), Mini Mental State Examination (MMSE; baseline, $F = 342.97$, $p < 0.001$; annual change, $F = 23.14$, $p < 0.001$), and Rey Auditory Verbal Learning Test (RAVLT; baseline, $F = 193.85$, $p < 0.001$; annual change, $F = 8.02$, $p < 0.001$). Paired comparisons between groups also indicated significant differences in both baseline values and annual change as shown in Table 1. No significant difference between groups was detected in baseline or 12-month age, gender distribution, handedness distribution, or baseline mean intracranial volume (ICV).

3.2. VBM comparisons

AD participants showed greater decline in global GM density than HCs (Fig. 1a, $p < 0.0001$ [uncorrected], k = 27) and MCI-S participants (Fig. 1d, $p < 0.0001$ [uncorrected], k = 27) in widespread regions including bilateral medial and lateral temporal lobe, frontal lobe, and parietal lobe, with maximal differences found in the left MTL. MCI-C participants also showed greater decline in global GM density relative to HCs (Fig. 1b, $p < 0.0001$ [uncorrected], k = 27) in bilateral medial and lateral temporal lobes, which was maximal in the left MTL (global peak). Differences in decline in GM density were also detected in bilateral hippocampal regions between HC and MCI-S participants and between MCI-C and MCI-S participants (Fig. 1c and 1e, $p < 0.0001$ [uncorrected], k = 27). Finally, greater decline in global GM density was detected for AD participants relative to MCI-C in a small cluster of voxels in the anterior parietal/posterior frontal lobe region (Fig. 1f, $p < 0.0001$ [uncorrected], k = 27).

3.3. Target region comparisons

Results from regional assessments of GM density and volume, as well as cortical thickness and volumetric measures, show a similar magnitude and anatomical pattern of decline over 12 months by group as seen in the results from the VBM comparisons. The APC values for all selected ROIs, including hippocampal GM density and GM volume extracted using 2 ROI methods (Brett et al., 2002; McHugh et al., 2007; Saykin et al., 2006; Shen et al., 2010), hippocampal volume, EC thickness, and mean lobar thickness values extracted using Freesurfer (Dale et al., 1999; Fischl and Dale, 2000a; Fischl et al., 1999; Fischl et al., 2002), and mean lobar GM density and GM volume extracted using MarsBaR ROIs (Brett et al., 2002) are found in Figs. 2–4 and Table 2. All APC values were significantly different across groups ($p < 0.001$). Significant posthoc paired comparisons using a Bonferroni correction are indicated in Table 2.

3.4. Sample sizes

The sample size needed to detect a 25% reduction in APC of MRI biomarkers was calculated for 80% or 90% power and a type I error (α) of $p < 0.05$ (Table 3). Mean bilateral hippocampal GM density and GM volume estimates measured using either the independent or MarsBaR ROIs would require the smallest sample size to detect the

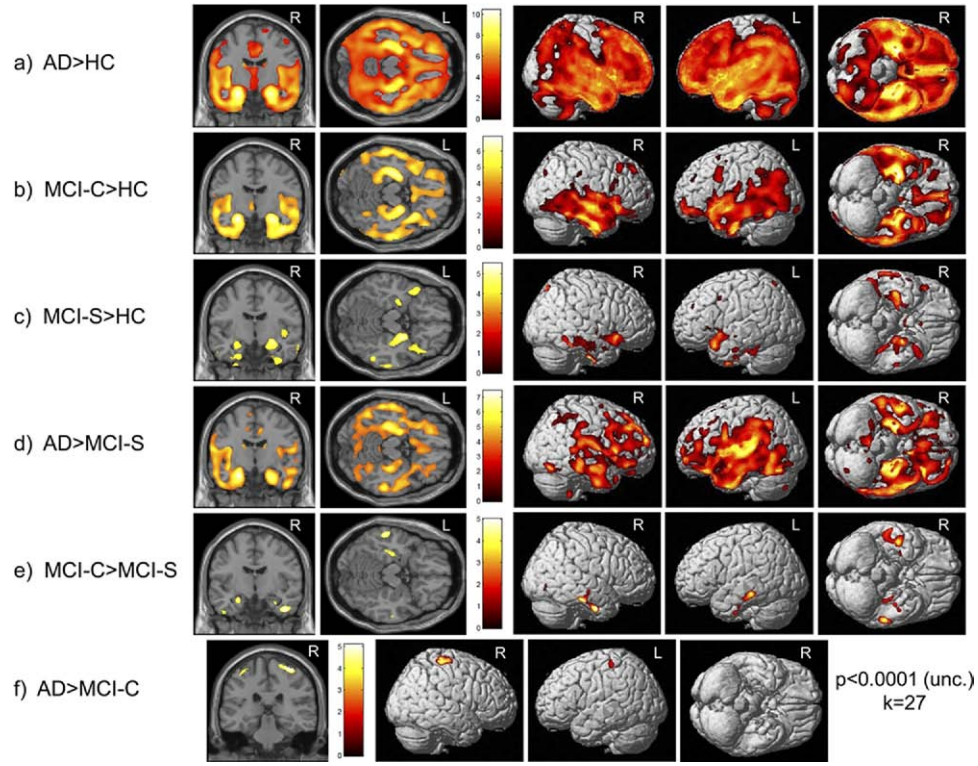

Fig. 1. Group differences in pattern of reduction in gray matter (GM) density over 12 months in the Alzheimer's Disease Neuroimaging Initiative (ADNI) cohort. Time × diagnosis group interactions demonstrate differences in atrophy progression reflected by reduction in GM density from baseline to 1 year in the ADNI cohort (n = 643 [30 participants removed from comparisons due to failed image processing]; 143 AD, 57 MCI-C, 253 MCI-S, 190 HC). Interaction contrasts are displayed at a threshold of $p < 0.0001$ (uncorrected) with a minimum cluster size (k) = 27 voxels. Cross-sections in (a–e) are (0, −9, 0, coronal) and (0, −23, −16, axial), left to right. Cross-section in (f) is (34, −29, 64, coronal). AD, Alzheimer's disease; HC, healthy control; MCI-C, converters from mild cognitive impairment to probable AD; MCI-S, mild cognitive impairment-stable.

desired reduction for all the target groups. Other relatively sensitive ROIs for detecting a reduction in regional brain atrophy include hippocampal volume extracted using Freesurfer, mean temporal lobar GM density and GM volume, mean temporal lobe cortical thickness (MCI-C only), and mean frontal lobar GM density and GM volume. A full list of sample sizes needed to detect a 25% decline in brain atrophy at either 80% or 90% power for selected ROIs is found in Table 3.

3.5. Effect sizes

In order to effectively compare the relative sensitivity of MRI markers to distinguish between groups, we calculated the effect size for all available baseline and APC ROIs from VBM and Freesurfer for each group pair. Effect sizes for the comparison of AD and HC participants and MCI-C and MCI-S participants are found in Fig. 5, while those for other pairs (MCI-C vs. HC; MCI-S vs. HC; AD vs. MCI-S; AD vs. MCI-C) are found in Supplementary Fig. 1. Baseline temporal lobe biomarkers, including EC thickness, hippocampal volume, and middle temporal gyri cortical thickness, had the highest effect sizes for the comparison of AD versus HC (Fig. 5a), with Cohen's d values of 1.846, 1.628, and 1.579, respectively. The APC in hippocampal GM density extracted using the MarsBaR ROIs had the highest effect size of the APC measures for AD versus HC with a Cohen's d of 1.308. Measures with maximal effect sizes for the comparison of MCI-C and MCI-S participants included APC in hippocampal GM volume (independent sample ROI, Cohen's d = 0.853; MarsBaR ROI, Cohen's d = 0.852), APC in inferior temporal gyri GM volume (Cohen's d = 0.842), and APC in mean temporal lobe GM volume (Cohen's d = 0.830). Temporal lobe ROIs also had high effect sizes for some of the other comparisons with baseline hippocampal volume showing the highest effect sizes for MCI-C versus HC (Suppl. Fig. 1a, Cohen's d = 1.652) and MCI-S versus HC (Suppl. Fig. 1b, Cohen's d = 0.958), and baseline middle temporal gyri thickness having the highest effect size for AD versus MCI-S (Suppl. Fig. 1c, Cohen's d = 0.890). APC in superior parietal gyri GM volume demonstrated the highest effect size for AD versus MCI-C with a Cohen's d of 0.456 (Suppl. Fig. 1d).

3.6. Influence of APOE ε4 genotype

The presence of one or more *APOE* ε4 alleles increased APC atrophy markers for hippocampal GM density (p = 0.001, Fig. 6a), hippocampal GM volume ($p < 0.001$; Fig. 6b), hippocampal volume (p = 0.001; Fig. 6c), and EC

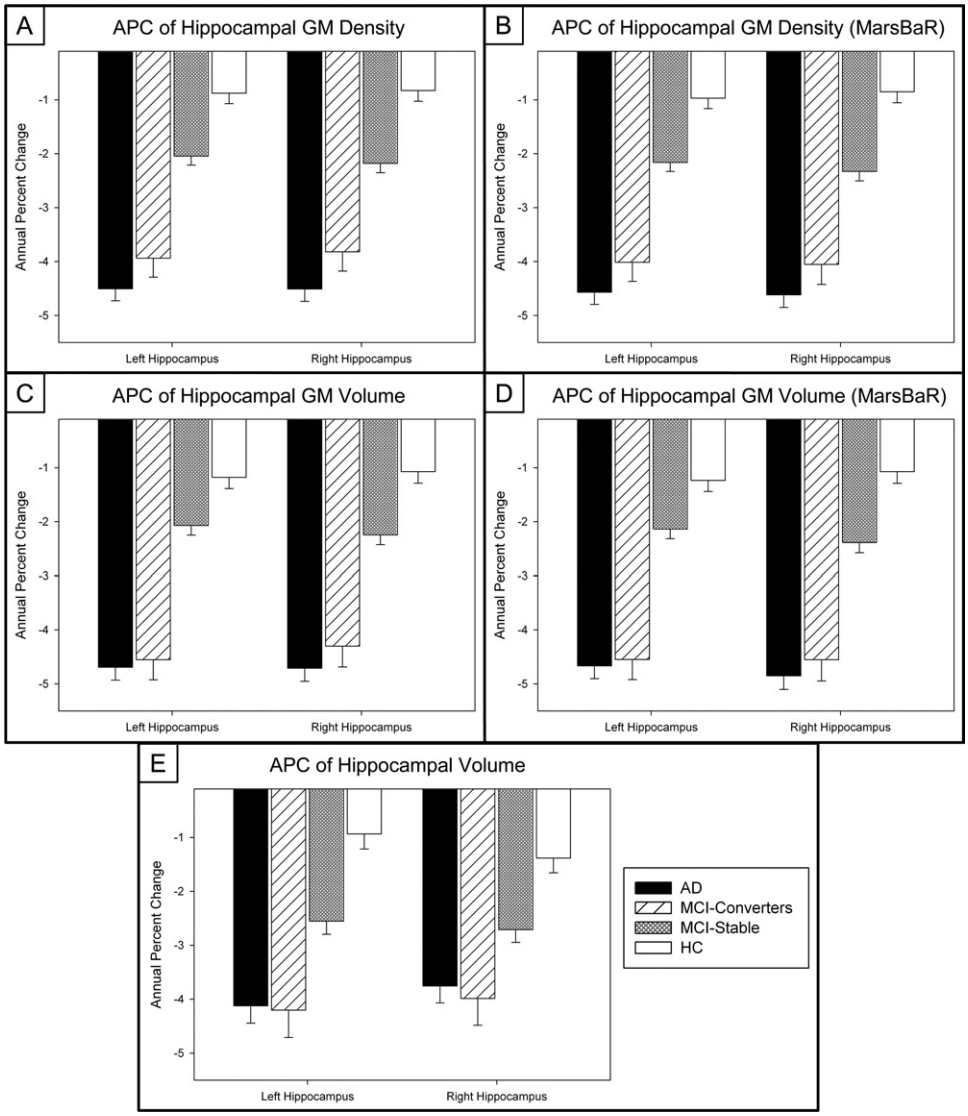

Fig. 2. Annual percent change (APC) of selected medial temporal lobe (MTL) imaging biomarkers. Plots of the mean APC in (A, B) hippocampal gray matter (GM) density and (C, D) GM volume extracted using a hippocampal region of interest (ROI) extracted using a template derived on an independent sample of 40 healthy elderly controls (McHugh et al., 2007; Saykin et al., 2006; Shen et al., 2010) and from MarsBaR, respectively ($n = 643$ [30 participants removed from comparisons due to failed image processing]; 143 AD, 57 MCI-C, 253 MCI-S, 190 HC). AD and MCI-C participants show significantly greater APC in hippocampal GM density and hippocampal GM volume relative to MCI-S and HC. The APC in (E) hippocampal volume ($n = 673$; 152 AD, 60 MCI-C, 261 MCI-S, 200 HC) extracted using Freesurfer (V4, http://surfer.nmr.mgh.harvard.edu/, Boston, MA) showed a similar trend. AD, Alzheimer's disease; HC, healthy control; MCI-C, converters from mild cognitive impairment to probable AD; MCI-S, mild cognitive impairment-stable.

thickness ($p = 0.003$; Fig. 6d). Additionally, a significant interaction between diagnosis group and *APOE* ε4 genotype was observed for the APC in EC thickness ($p = 0.029$). Subsequent analyses within diagnostic group demonstrated that for AD patients *APOE* ε4 carriers showed greater decline in hippocampal GM volume ($p = 0.031$) and EC thickness ($p = 0.002$). For MCI-C, *APOE* ε4 positive participants also showed greater rate of atrophy in hippocampal GM density ($p = 0.031$) and GM volume ($p = 0.001$). For the MCI-S group, the atrophy rate in all evaluated regions was greater in *APOE* ε4 positive than negative participants, including APCs for hippocampal GM density ($p = 0.004$), hippocampal GM volume ($p < 0.001$), hippocampal volume ($p = 0.006$), and EC thickness ($p = 0.004$). Finally, *APOE* ε4 positive HC participants showed a significantly greater APC in hippocampal volume than those who were *APOE* ε4 negative ($p = 0.004$).

4. Discussion

Our main goal was to assess a detailed panel of longitudinal MRI atrophy markers in the ADNI cohort, including patients with probable AD, MCI to AD converters (within 12 months), stable MCI (over 12 months), and control

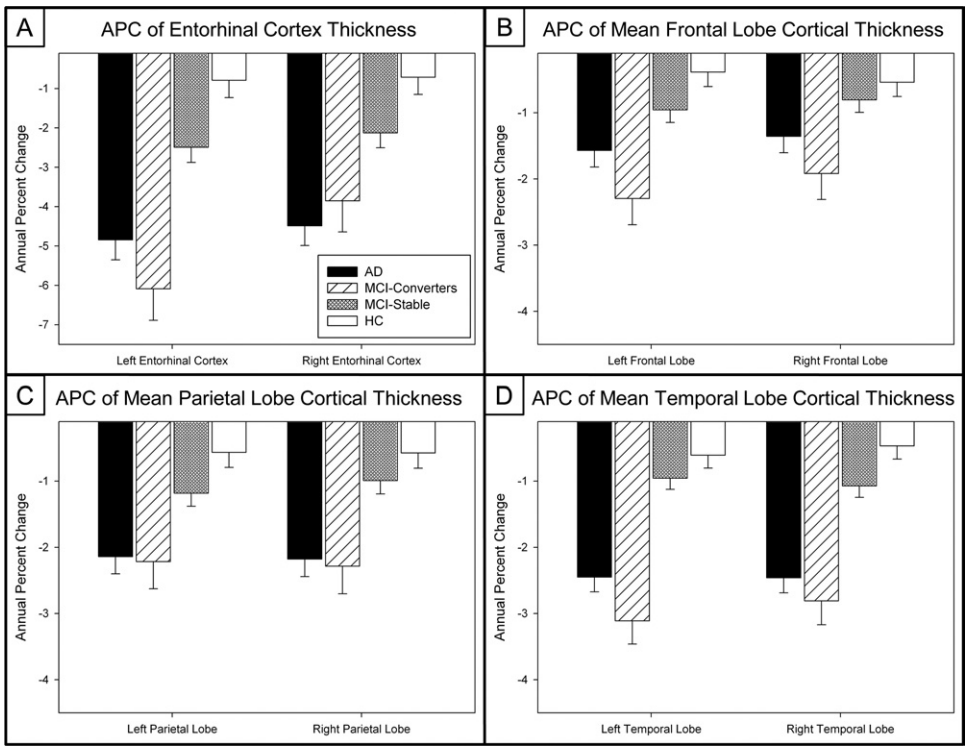

Fig. 3. Annual Percent Change (APC) of entorhinal cortex, mean frontal, parietal, and temporal lobe cortical thickness measures. APC in (A) entorhinal cortex thickness, and mean (B) frontal, (C) parietal, and (D) temporal lobar cortical thickness are significantly different across groups (n = 673; 152 AD, 60 MCI-C, 261 MCI-S, 200 HC). AD, Alzheimer's disease; HC, healthy control; MCI-C, converters from mild cognitive impairment to probable AD; MCI-S, mild cognitive impairment-stable.

participants. Our main findings were that AD and MCI-C groups had a significantly higher rate of annual decline in global and hippocampal GM density and GM volume, hippocampal total volume, EC thickness, and mean frontal, parietal and temporal lobar GM density, GM volume, and cortical thickness measures than MCI-S and HC participants. Sample size calculations indicated that hippocampal GM density and GM volume required the smallest samples to detect a 25% reduction in rate of regional brain atrophy. Finally, effect size estimates indicated that dynamic measures, including APC in MTL volumes and cortical thickness, showed the most discrimination between MCI-C and MCI-S participants. However, baseline hippocampal volume and GM density, as well as baseline temporal lobe cortical thickness measures, demonstrated the greatest effect size when comparing AD and HC participants. This pattern suggests that structural MRI markers may have differential utility as a function of stage of disease or role within a clinical trial. Whereas hippocampal volume and GM density are powerful tools for assessing baseline neurodegeneration, annual change rate in MTL volumes and cortical thickness may be most useful for comparing stable versus rapidly progressing individuals, and may be the best choice for surrogate markers in trials of disease-modifying agents.

Our estimates of APC in hippocampal volume, including −3.95% for AD patients, −4.10% for MCI-C participants, −2.65% for MCI-S participants, and −1.12% for HCs, were similar to estimates from previous reports in the ADNI cohort, as well as other samples (Table 2; Barnes et al., 2009). These results demonstrate a significantly accelerated rate of brain atrophy in participants diagnosed with AD, as well as those who show rapid clinical decline from MCI to AD. Participants who show stable clinical diagnoses (both MCI and HC) also show relatively stable brain volume and cortical thickness measures, as well as minimal change in psychometric variables (Table 1).

We examined the influence of *APOE* ε4 genotype on annual atrophy rate in selected MTL MRI markers given the mixed prior findings, including significant effects of *APOE* on brain atrophy in some reports (Jack et al., 2008c, 2008d), whereas others found no effect (Du et al., 2006; Wang et al., 2009). In the present study, we observed a modest but significant effect of *APOE* ε4 genotype on annualized hippocampal and EC atrophy rates. This effect was maximal in MCI-S participants, with ε4 positive participants demonstrating significantly greater APC in all measures evaluated. However, the effect of *APOE* genotype in AD and MCI-C groups was only observed on some measures, suggesting a more moderate yet still detectable effect of genotype. Fi-

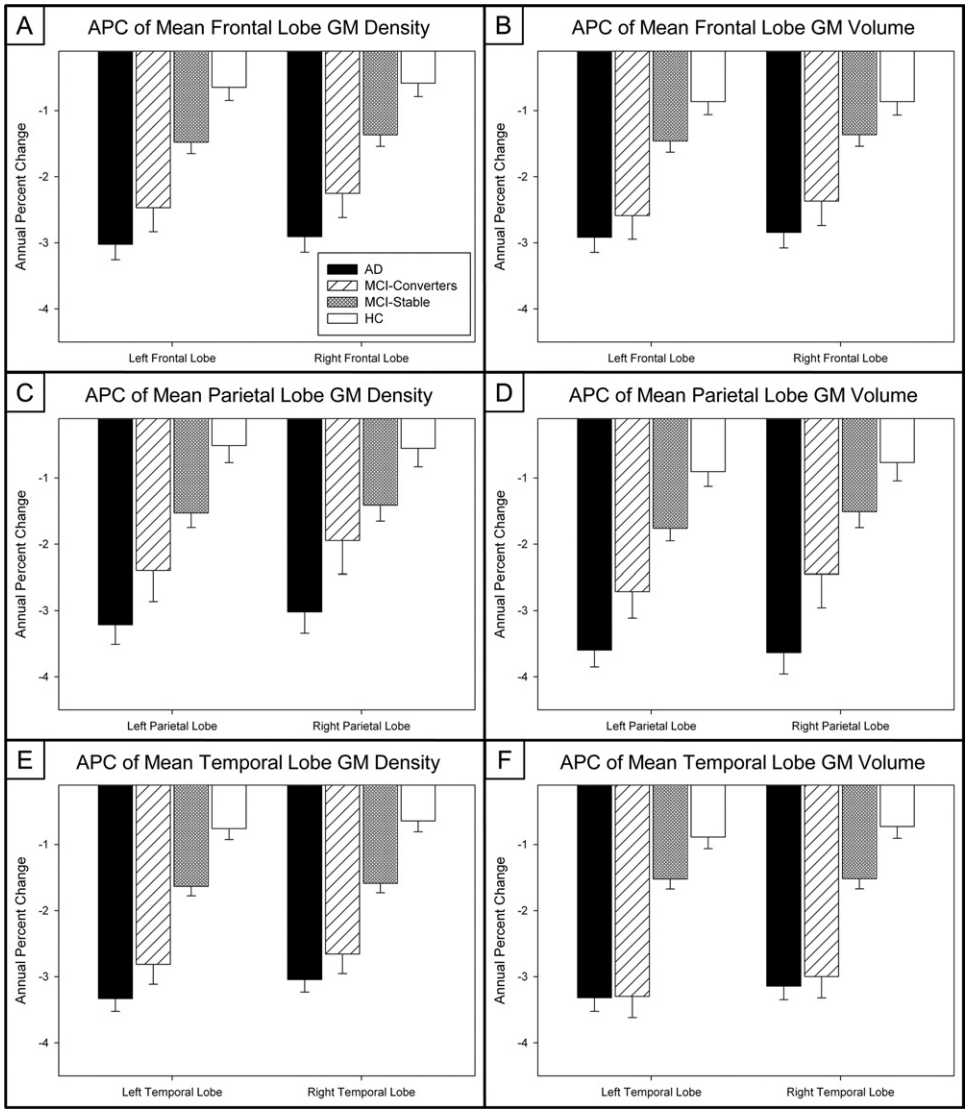

Fig. 4. Annual percent change (APC) of mean frontal, parietal, and temporal lobe gray matter (GM) density and volume measures. The APC in mean frontal lobe (A) GM density and (B) GM volume, mean parietal lobe (C) GM density and (D) GM volume, and mean temporal lobe (E) GM density and (F) GM volume are significantly different across groups (n = 643 [30 participants removed due to failed image processing]; 143 AD, 57 MCI-C, 253 MCI-S, 190 HC. AD, Alzheimer's disease; HC, healthy control; MCI-C, converters from mild cognitive impairment to probable AD; MCI-S, mild cognitive impairment-stable.

nally, *APOE* ε4 positive HC participants showed an enhanced rate of atrophy relative to ε4 negative participants only on hippocampal volume. Our results support the complicated nature of the relationship between *APOE* genotype and MRI markers of neurodegeneration and suggest that the magnitude of the effect may differ by diagnostic stage, as has been previously reported in the ADNI cohort (Nestor et al., 2008; Schuff et al., 2009). Future studies will further characterize the impact of *APOE*, as well as that of variation in other candidate genes, on MRI and other ADNI biomarkers which may assist in elucidating the role of genetic factors in the neuropathology of AD (Saykin et al., 2010).

This report adds to the body of research demonstrating the utility of MRI metrics in detecting and monitoring atrophy associated with AD and MCI, and extends prior research by focusing on identifying differences between rapidly declining MCI to AD converters and individuals with relatively stable MCI. Reports in other smaller samples have led to similar conclusions regarding the utility of MRI extracted measures of global and local brain volume, cortical thickness, and morphometry in detecting and monitoring brain atrophy associated with AD and MCI (Barnes et al., 2007; Cardenas et al., 2003; Erten-Lyons et al., 2006; Fox and Freeborough, 1997; Jack et al., 2000, 2004, 2005; Mungas et al., 2005; Sluimer et al., 2008; Stoub et al., 2008; Thompson et al., 2004; Whitwell et al., 2008a). As previously reported in the ADNI sample, baseline values of hippocampal GM density and volume, amygdalar volume,

Table 2
APC of selected imaging biomarkers

		AD (n = 152)	MCI-C (n = 60)	MCI-S (n = 261)	HC (n = 200)	p-value	Significant pair comparisons ($p < 0.05$)
Hippocampal GM density (independent ROI)[a,b]	L:	−4.51 (0.2)	−3.94 (0.4)	−2.05 (0.2)	−0.88 (0.2)	$p < 0.001$	HC > MCI-S > MCI-C, AD
	R:	−4.51 (0.2)	−3.82 (0.4)	−2.18 (0.2)	−0.83 (0.2)	$p < 0.001$	HC > MCI-S > MCI-C, AD
Hippocampal GM density (MarsBaR)[a,b]	L:	−4.57 (0.2)	−4.02 (0.4)	−2.16 (0.2)	−0.97 (0.2)	$p < 0.001$	HC > MCI-S > MCI-C, AD
	R:	−4.62 (0.2)	−4.05 (0.4)	−2.33 (0.2)	−0.85 (0.2)	$p < 0.001$	HC > MCI-S > MCI-C, AD
Hippocampal GM volume (independent ROI)[a,b]	L:	−4.69 (0.2)	−4.55 (0.4)	−2.07 (0.2)	−1.18 (0.2)	$p < 0.001$	HC > MCI-S > MCI-C, AD
	R:	−4.71 (0.2)	−4.30 (0.4)	−2.25 (0.2)	−1.07 (0.2)	$p < 0.001$	HC > MCI-S > MCI-C, AD
Hippocampal GM volume (MarsBaR)[a,b]	L:	−4.67 (0.2)	−4.55 (0.4)	−2.14 (0.2)	−2.24 (0.2)	$p < 0.001$	HC > MCI-S > MCI-C, AD
	R:	−4.85 (0.3)	−4.55 (0.4)	−2.39 (0.2)	−1.07 (0.2)	$p < 0.001$	HC > MCI-S > MCI-C, AD
Hippocampal volume (Freesurfer)[b]	L:	−4.12 (0.3)	−4.20 (0.5)	−2.55 (0.2)	−0.94 (0.3)	$p < 0.001$	HC > MCI-S > MCI-C, AD
	R:	−3.76 (0.3)	−3.99 (0.5)	−2.71 (0.2)	−1.38 (0.3)	$p < 0.001$	HC > MCI-S, MCI-C, AD
EC thickness (Freesurfer)[b]	L:	−4.84 (0.5)	−6.09 (0.8)	−2.49 (0.4)	−0.79 (0.4)	$p < 0.001$	HC > MCI-S > MCI-C, AD
	R:	−4.49 (0.5)	−3.85 (0.8)	−2.16 (0.4)	−0.71 (0.4)	$p < 0.001$	HC > MCI-C, AD; MCI-S > AD
Mean frontal cortical thickness (Freesurfer)[b]	L:	−1.57 (0.3)	−2.30 (0.4)	−0.96 (0.2)	−0.39 (0.2)	$p < 0.001$	HC, MCI-S > MCI-C; HC > AD
	R:	−1.36 (0.2)	−1.92 (0.4)	−0.81 (0.2)	−0.54 (0.2)	$p = 0.006$	HC > MCI-C
Mean parietal cortical thickness (Freesurfer)[b]	L:	−2.14 (0.3)	−2.22 (0.4)	−1.18 (0.2)	−0.57 (0.2)	$p < 0.001$	HC > MCI-C, AD; MCI-S > AD
	R:	−2.18 (0.3)	−2.28 (0.4)	−0.99 (0.2)	−0.58 (0.2)	$p < 0.001$	HC, MCI-S > MCI-C, AD
Mean temporal cortical thickness (Freesurfer)[b]	L:	−2.45 (0.2)	−3.11 (0.4)	−0.96 (0.2)	−0.61 (0.2)	$p < 0.001$	HC, MCI-S > MCI-C, AD
	R:	−2.46 (0.2)	−2.81 (0.4)	−1.07 (0.2)	−0.47 (0.2)	$p < 0.001$	HC, MCI-S > MCI-C, AD
Mean frontal GM density (MarsBaR)[a,b]	L:	−3.02 (0.2)	−2.47 (0.4)	−1.48 (0.2)	−0.65 (0.2)	$p < 0.001$	HC > MCI-S > AD; HC > MCI-C
	R:	−2.91 (0.2)	−2.25 (0.4)	−1.37 (0.2)	−0.59 (0.2)	$p < 0.001$	HC > MCI-S > AD; HC > MCI-C
Mean frontal GM volume (MarsBaR)[a,b]	L:	−2.92 (0.2)	−2.59 (0.4)	−1.46 (0.2)	−0.86 (0.2)	$p < 0.001$	HC, MCI-S > MCI-C, AD
	R:	−2.84 (0.2)	−2.37 (0.4)	−1.36 (0.2)	−0.86 (0.2)	$p < 0.001$	HC > MCI-S > AD; HC > MCI-C
Mean parietal GM density (MarsBaR)[a,b]	L:	−3.21 (0.3)	−2.40 (0.5)	−1.53 (0.2)	−0.51 (0.3)	$p < 0.001$	HC > MCI-S > AD; HC > MCI-C
	R:	−3.02 (0.3)	−1.95 (0.5)	−1.41 (0.2)	−0.55 (0.3)	$p < 0.001$	HC, MCI-S > AD
Mean parietal GM volume (MarsBaR)[a,b]	L:	−3.60 (0.3)	−2.71 (0.4)	−1.76 (0.2)	−0.90 (0.2)	$p < 0.001$	HC > MCI-S > AD; HC > MCI-C
	R:	−3.64 (0.3)	−2.45 (0.5)	−1.51 (0.2)	−0.76 (0.3)	$p < 0.001$	HC > MCI-S > AD; HC > MCI-C
Mean temporal GM density (MarsBaR)[a,b]	L:	−3.33 (0.2)	−2.81 (0.3)	−1.63 (0.1)	−0.76 (0.2)	$p < 0.001$	HC > MCI-S > MCI-C, AD
	R:	−3.04 (0.2)	−2.66 (0.3)	−1.59 (0.1)	−0.64 (0.2)	$p < 0.001$	HC > MCI-S > MCI-C, AD
Mean temporal GM volume (MarsBaR)[a,b]	L:	−3.32 (0.2)	−3.30 (0.3)	−1.52 (0.2)	−0.89 (0.2)	$p < 0.001$	HC > MCI-S > MCI-C, AD
	R:	−3.14 (0.2)	−3.00 (0.3)	−1.52 (0.2)	−0.73 (0.2)	$p < 0.001$	HC > MCI-S > MCI-C, AD

Data are given as mean (standard error of the mean).
Key: AD, Alzheimer's disease; APC, annual percent change; EC, entorhinal cortex; GM, gray matter; HC, healthy control; MCI-C, converters from mild cognitive impairment to probable AD; MCI-S, mild cognitive impairment-stable; ROI, region of interest.
[a] 30 participants excluded because of failed processing (9 AD, 3 MCI-C, 9 MCI-S, 9 HC).
[b] Covaried for baseline age, gender, education, handedness, and baseline intracranial volume (ICV).

EC thickness, and temporal and parietal lobe cortical thickness measures are significantly different between MCI-C and MCI-S participants (Risacher et al., 2009). In fact, MCI-C and AD participants show nearly equivalent atrophy at baseline, up to 12 months prior to equivalent clinical diagnoses, indicating that MRI can serve as an antecedent biomarker. Measures of annual decline provide further evidence that MCI to AD converters have characteristic cross-sectional and longitudinal brain atrophy more similar to AD patients than to those with stable MCI. The different longitudinal phenotypes warrant investigation and may be useful in examining genetic variation associated with rate of decline (Jack et al., 2008c; Saykin et al., 2009).

Our results are generally consistent with previous reports using subsets of the ADNI cohort and alternative methods. Four studies employed Freesurfer-based ROI techniques to estimate APC in selected cortical and subcortical regions and reported similar APC values and differences between diagnostic groups as those observed in the present analysis (Fjell et al., 2010b; Holland et al., 2009; McDonald et al., 2009; McEvoy et al., 2009). Furthermore, two of these studies divided the MCI group by baseline Clinical Dementia Rating-Sum of Boxes (CDR-SB) (McDonald et al., 2009) and by atrophy pattern (AD-like vs. HC-like; McEvoy et al., 2009) and showed variability of APC values within the MCI group, similar to that seen in the present report between MCI-C and MCI-S participants. Two studies used various hippocampal ROIs and reported significantly greater APC in hippocampal volume in AD participants relative to MCI and HC participants (Morra et al., 2009; Schuff et al., 2009). Two studies examined changes in ventricular volume, demonstrating greater rates of ventricular enlargement in AD and MCI participants relative to HCs, as well as greater ventricular enlargement in participants who converted from MCI to AD within the first 6 months of the study relative to MCI-S participants (Jack et al., 2009; Nestor et al., 2008). Three additional studies employed TBM and Jacobian maps to investigate whole brain and temporal lobe atrophy rates and found a similar pattern of differences between participants as seen in the present study (Ho et al., 2009; Hua et al., 2009; Leow et al., 2009). One of these studies also reported a higher rate of atrophy in MCI-C relative to MCI-S participants, albeit in a

Table 3
Sample sizes to detect 25% reduction in APC of selected MRI biomarkers

	AD		MCI-C		MCI-S		HC	
Power:	0.8	0.9	0.8	0.9	0.8	0.9	0.8	0.9
Hippocampal GM density (independent ROI)	134	180	95	128	307	411	1243	1665
Hippocampal GM density (MarsBaR ROI)	129	173	96	129	290	388	1204	1612
Hippocampal GM volume (independent ROI)	133	178	77	103	400	535	745	998
Hippocampal GM volume (MarsBaR ROI)	135	181	74	100	378	507	767	1028
Hippocampal volume (Freesurfer)	242	324	129	173	452	606	1136	1521
EC thickness (Freesurfer)	328	439	214	286	1156	1548	7948	10,648
Mean frontal lobe cortical thickness (FreeSurfer)	1037	1389	369	494	2488	3333	4727	6333
Mean parietal lobe cortical thickness (Freesurfer)	629	842	515	689	1848	2475	3142	4209
Mean temporal lobe cortical thickness (Freesurfer)	403	539	121	162	1405	1882	3031	4061
Mean frontal lobe GM density (MarsBaR ROIs)	284	381	222	297	788	1056	3682	4932
Mean frontal lobe GM volume (MarsBaR ROIs)	280	376	263	353	856	1147	1475	1976
Mean parietal lobe GM density (MarsBaR ROIs)	384	514	373	499	1437	1925	7260	9726
Mean parietal lobe GM volume (MarsBaR ROIs)	238	319	315	422	976	1308	1977	2649
Mean temporal lobe GM density (MarsBaR ROIs)	157	210	129	173	456	610	1850	2479
Mean temporal lobe GM volume (MarsBaR ROIs)	158	212	100	134	646	866	1427	1911

Key: AD, Alzheimer's disease; APC, annual percent change; EC, entorhinal cortex; GM, gray matter; HC, healthy control; MCI-C, converters from mild cognitive impairment to probable AD; MCI-S, mild cognitive impairment-stable; MRI, magnetic resonance imaging; ROI, region of interest.

significantly smaller sample (7 MCI-C and 32 MCI-S) than used in the present analysis (Leow et al., 2009). Misra et al. (2009) also reported significant differences in atrophy rate between MCI-C and MCI-S participants using a VBM-like technique (RAVENS), although differences were limited to periventricular white matter and the temporal horn (Misra et al., 2009). Finally, another study used a boundary shift integral (BSI) technique to evaluate annual rates of whole brain atrophy and ventricular enlargement (Evans et al., 2009). This study reported greater annual rates of whole brain atrophy and ventricular enlargement in AD participants relative to MCI and HC participants, as well as in MCI-C relative to MCI-S participants. In fact, Evans et al. (2009) noted that MCI-C participants demonstrated nearly equivalent rates of atrophy as seen in the AD participants, similar to the pattern reported in the present study. Overall, the results of the present study extend this line of research by providing one of the first direct comparisons of annual atrophy rates for an ensemble of state-of-the-art MRI morphometric, volumetric, and cortical thickness variables in the ADNI cohort, particularly focusing on participants who converted from MCI to AD within the first 12 months of the study.

There are several limitations of the present study. First, we were unable to account for some other variables which may have impacted the results. Because the ADNI is an observational study, many participants were taking a number of medications prescribed for AD, MCI, or other conditions that could have affected the results. Additionally, differences in disease severity beyond clinical diagnostic classification (i.e., AD, MCI, HC) was not considered in the present analyses. Although diagnostic classification and conversion status incorporates information from psychometric performance, the present report does not explicitly examine the relationship between changes in MRI variables and changes in psychometric performance. Secondly, the inclusion of only 2 time points separated by approximately 1 year in the present study limited the specificity and accuracy of the APC estimations. One of the major advantages of the ADNI project is the extensive longitudinal data collection. Therefore, as full datasets from the 2- and 3-year time points become available, we plan to expand our analysis of annual atrophy rates in patients with AD, MCI converters, MCI stables, and healthy elderly. Furthermore, we will employ more advanced statistical modeling to compare the atrophy rates between MCI-C participants from several time points. With 3 or more time points nonlinearities can be detected. Finally, this study was limited by the nature of the methods employed to measure atrophy. Specifically, some variability in segmentation and extraction of ROIs is likely, based on the interaction between scan quality or other properties and specific image processing algorithms which may have resulted in variation in the accuracy of the annual change estimates. However, the largely automated methodology employed in these analyses provides for little or no rater bias inherent in manually-directed tools of volume extraction. Furthermore, other analysis techniques (e.g., TBM, BSI) may provide additional and complementary information to that extracted in the present study using VBM and automated parcellation. Although a comprehensive and direct comparison of the relative sensitivity and specificity of target MRI-based atrophy measures extracted using different methods has not been completed to our knowledge, ADNI provides an ideal cohort for investigating this issue. Finally, better methods for visualization and display of longitudinal changes on a voxel-wise basis would also be advantageous. Statistical parametric maps of time by group interactions, like those presented in the present study, do not illustrate the percent change at all significant locations. Development of improved tools for visualization of magnitude of changes as a function of diagnostic group would be useful.

In summary, this study used a combination of analysis methods to confirm that MRI-based morphometric markers

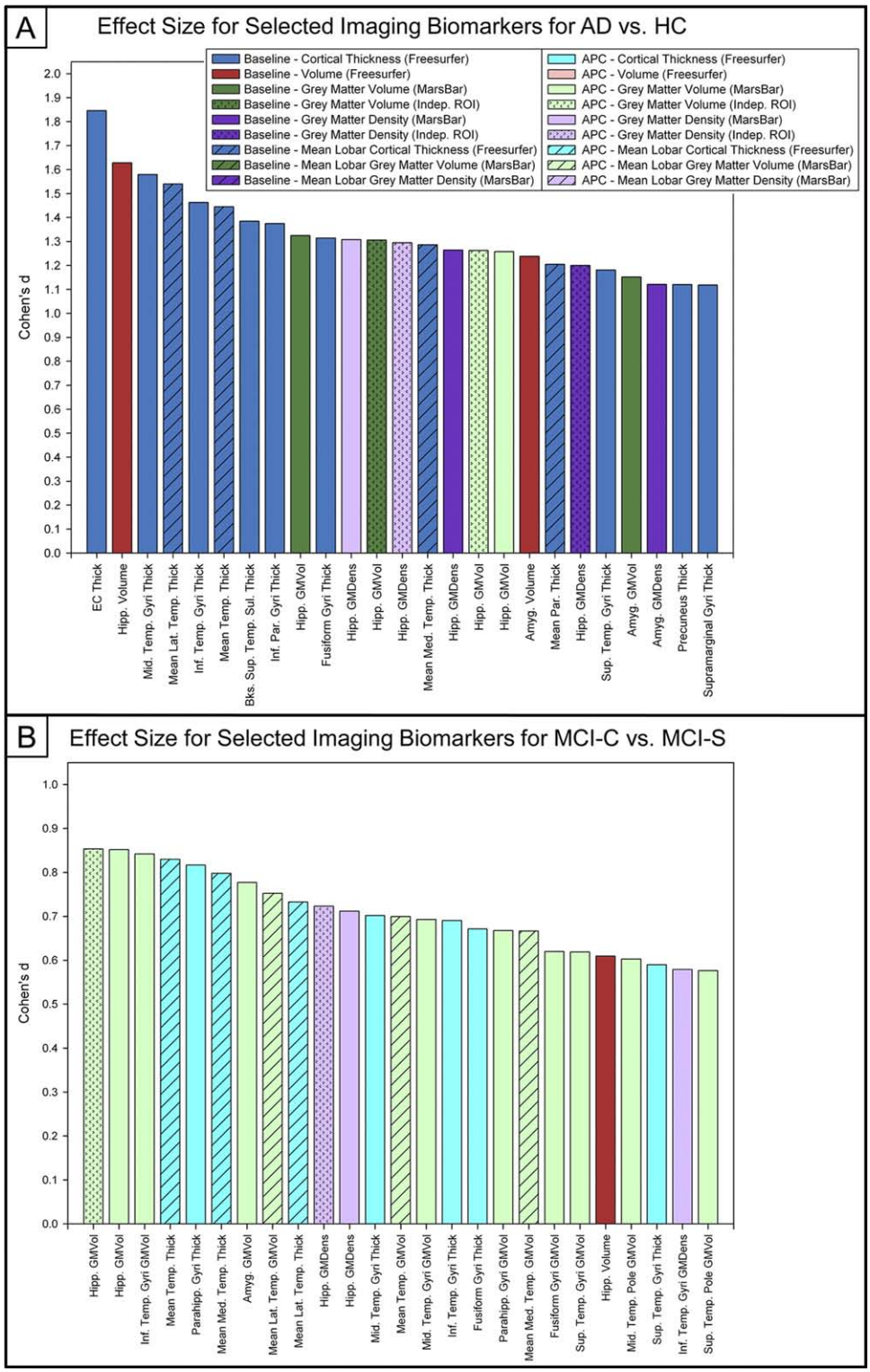

Fig. 5. Effect sizes of comparisons between AD and HC, and MCI-C and MCI-S for selected imaging biomarkers. The effect sizes for selected baseline and annual percent change (APC) values for the comparison of (A) AD and HC participants and (B) MCI-C and MCI-S participants are shown. Baseline medial temporal lobe (MTL) regions had the greatest effect sizes when comparing AD and HC, while APC in MTL regions demonstrated the greatest effect sizes in the MCI-C versus MCI-S comparison (n = 643 [30 participants removed due to failed image processing]; 143 AD, 57 MCI-C, 253 MCI-S, 190 HC). AD, Alzheimer's disease; HC, healthy control; MCI-C, converters from mild cognitive impairment to probable AD; MCI-S, mild cognitive impairment-stable.

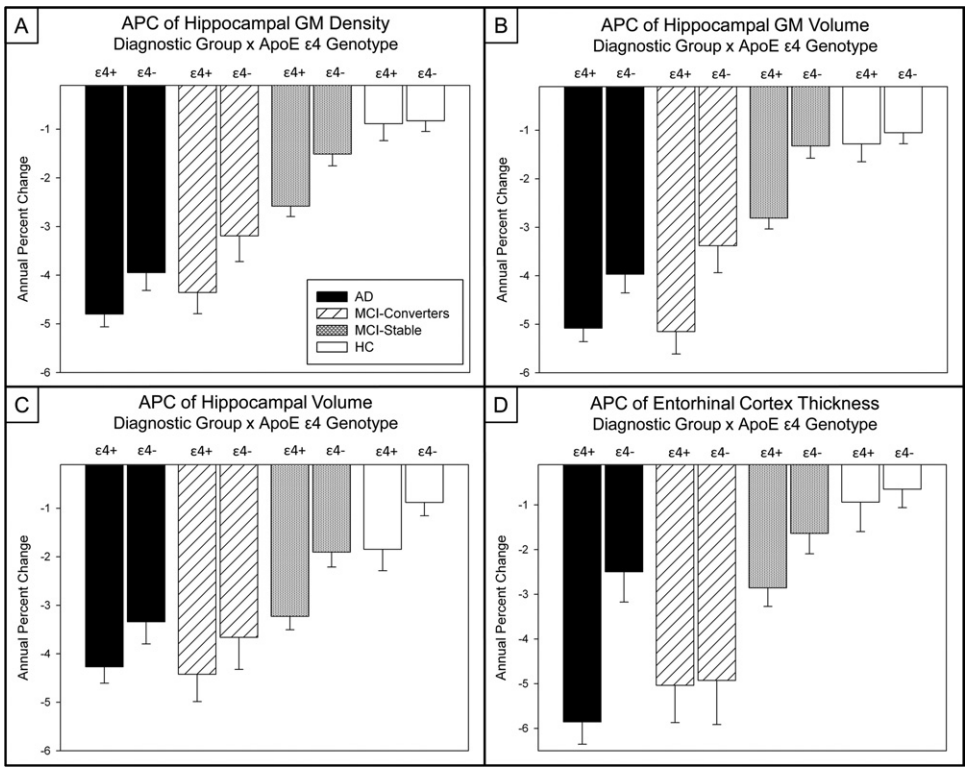

Fig. 6. Impact of *APOE* ε4 genotype on annual percent change (APC) of selected medial temporal lobe (MTL) measures. The APC in bilateral mean hippocampal (A) gray matter (GM) density and (B) GM volume (n = 643 [30 participants removed due to failed image processing]; 143 AD, 57 MCI-C, 253 MCI-S, 190 HC), extracted using an independent sample of 40 healthy elderly controls (McHugh et al., 2007; Saykin et al., 2006; Shen et al., 2010), as well as (C) hippocampal volume, and (D) entorhinal cortex (EC) thickness extracted using automated parcellation (n = 673; 152 AD, 60 MCI-C, 261 MCI-S, 200 HC) show a significant effect of both diagnostic group and *APOE* ε4 genotype. AD, Alzheimer's disease; HC, healthy control; MCI-C, converters from mild cognitive impairment to probable AD; MCI-S, mild cognitive impairment-stable.

detect dynamic changes in rate of atrophy in patients with AD and MCI, compared with controls, and are highly sensitive to the likelihood of clinical progression within 1 year. Measures of GM density change within medial and lateral temporal regions have been employed less than volumetric measures to date but appear particularly promising and complementary to more standard measures such as hippocampal volumetry. The sensitivity of automated and unbiased methods for detecting differences in rate of neurodegenerative changes encourages their use in clinical trials of disease-modifying agents and in prevention trials.

Disclosure statement

Drs. Risacher, Shen, Kim, West, McDonald, Beckett, and Harvey report no disclosures. Dr. Jack served on a scientific advisory board for Elan Corporation; receives research support from Pfizer Inc., the Mayo U of MN Biotechnology Partnership, and holds stock in GE Healthcare. Dr. Weiner serves on scientific advisory boards for Bayer Schering Pharma, Eli Lilly and Company, CoMentis, Inc., Neurochem Inc, Eisai Inc., Avid Radiopharmaceuticals Inc., Aegis Therapies, Genentech, Inc., Allergan, Inc., Lippincott Williams & Wilkins, Bristol-Myers Squibb, Forest Laboratories, Inc., Pfizer Inc, McKinsey & Company, Mitsubishi, Tanabe Pharma Corporation, and Novartis; has received funding for travel from Nestle and Kenes International and to attend conferences not funded by industry; has received honoraria from the Rotman Research Institute and BOLT International; serves as a consultant for Elan Corporation; receives research support from Merck & Co., Radiopharmaceuticals Inc., and holds stock in Synarc and Elan Corporation. Dr. Saykin receives support from the NIH (R01 CA101318, R01 AG19771, RC2 AG036535, P30 AG10133-18S1, U01 AG032984), Indiana Economic Development Corporation (IEDC # 87884), and from Siemens Medical Solutions and Welch Allyn, Inc.Informed consent was obtained from all ADNI participants according to the Helsinki Declaration and necessary approval was received from Ethical Committees at each of the participating research institutions. Further information about ADNI can be found in (Jack et al., 2008a; Mueller et al., 2005; Petersen et al., 2010a) and at www.adni-info.org.

Acknowledgements

Data used in the preparation of this article were obtained from the Alzheimer's Disease Neuroimaging Initiative

(ADNI) database (www.loni.ucla.edu/ADNI). As such, the investigators within the ADNI contributed to the design and implementation of ADNI and/or provided data but did not participate in analysis or writing of this report. For a complete list of investigators involved in ADNI see: http://www.loni.ucla.edu/ADNI/Data/ADNI_Authorship_List.pdf.

Data collection and sharing for this project was funded by the Alzheimer's Disease Neuroimaging Initiative (ADNI; National Institutes of Health, Grants U01 AG024904 and RC2 AG036535, PI: Michael W. Weiner, MD). ADNI is funded by the National Institute on Aging, the National Institute of Biomedical Imaging and Bioengineering, and through generous contributions from the following: Abbott, AstraZeneca AB, Bayer Schering Pharma AG, Bristol-Myers Squibb, Eisai Global Clinical Development, Elan Corporation, Genentech, GE Healthcare, GlaxoSmithKline, Innogenetics, Johnson and Johnson, Eli Lilly and Co., Medpace, Inc., Merck and Co., Inc., Novartis AG, Pfizer Inc, F. Hoffman-La Roche, Schering-Plough, Synarc, Inc., and Wyeth, as well as nonprofit partners the Alzheimer's Association and Alzheimer's Drug Discovery Foundation, with participation from the US Food and Drug Administration. Private sector contributions to ADNI are facilitated by the Foundation for the National Institutes of Health (www.fnih.org). The grantee organization is the Northern California Institute for Research and Education, and the study is coordinated by the Alzheimer's Disease Cooperative Study at the University of California, San Diego. ADNI data are disseminated by the Laboratory for Neuro Imaging at the University of California, Los Angeles. This research was also supported by NIH grants P30 AG010129, K01 AG030514, and the Dana Foundation. The National Cell Repository for Alzheimer's Disease (NIH grant U24 AG021886) provided support for DNA and cell line banking and processing for ADNI.

Data analysis was supported in part by the following grants from the National Institutes of Health: NIA R01 AG19771 to AJS and P30 AG10133-18S1 to B. Ghetti and AJS, and NIBIB R03 EB008674 to LS; and by the Indiana Economic Development Corporation (IEDC # 87884 to AJS).

The Freesurfer analyses were performed on a 112-node parallel computing environment called Quarry at Indiana University. We thank the University Information Technology Services at Indiana University and Randy Heiland, MA, MS, for their support.

Appendix. Supplementary data

Supplementary data associated with this article can be found, in the online version, at doi:10.1016/j.neurobiolaging.2010.04.029.

References

Apostolova, L., Dutton, R., Dinov, I., Hayashi, K., Toga, A., Cummings, J., Thompson, P., 2006. Conversion of mild cognitive impairment to Alzheimer disease predicted by hippocampal atrophy maps. Arch. Neurol. 63, 693–699.

Ashburner, J., Friston, K.J., 2000. Voxel-based morphometry − the methods. Neuroimage 11, 805–821.

Barnes, J., Bartlett, J.W., van de Pol, L.A., Loy, C.T., Scahill, R.I., Frost, C., Thompson, P., Fox, N.C., 2009. A meta-analysis of hippocampal atrophy rates in Alzheimer's disease. Neurobiol. Aging 30, 1711–1723.

Barnes, J., Boyes, R.G., Lewis, E.B., Schott, J.M., Frost, C., Scahill, R.I., Fox, N.C., 2007. Automatic calculation of hippocampal atrophy rates using a hippocampal template and the boundary shift integral. Neurobiol. Aging 28, 1657–1663.

Becker, J.T., Davis, S.W., Hayashi, K.M., Meltzer, C.C., Toga, A.W., Lopez, O.L., Thompson, P.M., 2006. Three-dimensional patterns of hippocampal atrophy in mild cognitive impairment. Arch. Neurol. 63, 97–101.

Bertram, L., Tanzi, R.E., 2008. Thirty years of Alzheimer's disease genetics: the implications of systematic meta-analyses. Nat. Rev. Neurosci. 9, 768–778.

Bozzali, M., Filippi, M., Magnani, G., Cercignani, M., Franceschi, M., Schiatti, E., Castiglioni, S., Mossini, R., Falautano, M., Scotti, G., Comi, G., Falini, A., 2006. The contribution of voxel-based morphometry in staging patients with mild cognitive impairment. Neurology 67, 453–460.

Brett, M., Anton, J.-L., Valabregue, R., Poline, J.-B., 2002. Region of interest analysis using an SPM toolbox [Abstract]. Presented At The 8th International Conference on Functional Mapping of the Human Brain, June, pp. 2–6, 2002, Sendai, Japan.

Busatto, G.F., Garrido, G.E., Almeida, O.P., Castro, C.C., Camargo, C.H., Cid, C.G., Buchpiguel, C.A., Furuie, S., Bottino, C.M., 2003. A voxel-based morphometry study of temporal lobe gray matter reductions in Alzheimer's disease. Neurobiol. Aging 24, 221–231.

Calvini, P., Chincarini, A., Gemme, G., Penco, M.A., Squarcia, S., Nobili, F., Rodriguez, G., Bellotti, R., Catanzariti, E., Cerello, P., De Mitri, I., Fantacci, M.E., 2009. Automatic analysis of medial temporal lobe atrophy from structural MRIs for the early assessment of Alzheimer disease. Med. Phys. 36, 3737–3747.

Cardenas, V.A., Du, A.T., Hardin, D., Ezekiel, F., Weber, P., Jagust, W.J., Chui, H.C., Schuff, N., Weiner, M.W., 2003. Comparison of methods for measuring longitudinal brain change in cognitive impairment and dementia. Neurobiol. Aging 24, 537–544.

Chetelat, G., Desgranges, B., De La Sayette, V., Viader, F., Eustache, F., Baron, J.C., 2002. Mapping gray matter loss with voxel-based morphometry in mild cognitive impairment. Neuroreport 13, 1939–1943.

Chetelat, G., Landeau, B., Eustache, F., Mezenge, F., Viader, F., de la Sayette, V., Desgranges, B., Baron, J.C., 2005. Using voxel-based morphometry to map the structural changes associated with rapid conversion in MCI: a longitudinal MRI study. Neuroimage 27, 934–946.

Chou, Y.Y., Lepore, N., Avedissian, C., Madsen, S.K., Parikshak, N., Hua, X., Shaw, L.M., Trojanowski, J.Q., Weiner, M.W., Toga, A.W., Thompson, P.M., 2009. Mapping correlations between ventricular expansion and CSF amyloid and tau biomarkers in 240 subjects with Alzheimer's disease, mild cognitive impairment and elderly controls. Neuroimage 46, 394–410.

Chupin, M., Gerardin, E., Cuingnet, R., Boutet, C., Lemieux, L., Lehericy, S., Benali, H., Garnero, L., Colliot, O., 2009. Fully automatic hippocampus segmentation and classification in Alzheimer's disease and mild cognitive impairment applied on data from ADNI. Hippocampus 19, 579–587.

Cohen, J., 1988. Statistical Power Analysis for the Behavioral Sciences, 2nd Ed. Lawrence Erlbaum Associates, Hillsdale, NJ.

Cohen, R.M., Small, C., Lalonde, F., Friz, J., Sunderland, T., 2001. Effect of apolipoprotein E genotype on hippocampal volume loss in aging healthy women. Neurology 57, 2223–2228.

Colliot, O., Chetelat, G., Chupin, M., Desgranges, B., Magnin, B., Benali, H., Dubois, B., Garnero, L., Eustache, F., Lehericy, S., 2008. Discrim-

ination between Alzheimer disease, mild cognitive impairment, and normal aging by using automated segmentation of the hippocampus. Radiology 248, 194–201.

Dale, A., Fischl, B., Sereno, M., 1999. Cortical surface-based analysis. I. Segmentation and surface reconstruction. Neuroimage 9, 179–194.

de Leon, M.J., Mosconi, L., Blennow, K., DeSanti, S., Zinkowski, R., Mehta, P.D., Pratico, D., Tsui, W., Saint Louis, L.A., Sobanska, L., Brys, M., Li, Y., Rich, K., Rinne, J., Rusinek, H., 2007. Imaging and CSF studies in the preclinical diagnosis of Alzheimer's disease. Ann. N. Y. Acad. Sci. 1097, 114–145.

De Toledo-Morrell, L., Goncharova, I., Dickerson, B., Wilson, R.S., Bennett, D.A., 2000. From healthy aging to early Alzheimer's disease: in vivo detection of entorhinal cortex atrophy. Ann. N.Y. Acad. Sci. 911, 240–253.

Devanand, D.P., Pradhaban, G., Liu, X., Khandji, A., De Santi, S., Segal, S., Rusinek, H., Pelton, G.H., Honig, L.S., Mayeux, R., Stern, Y., Tabert, M.H., de Leon, M.J., 2007. Hippocampal and entorhinal atrophy in mild cognitive impairment: prediction of Alzheimer disease. Neurology 68, 828–836.

Dickerson, B.C., Goncharova, I., Sullivan, M.P., Forchetti, C., Wilson, R.S., Bennett, D.A., Beckett, L.A., deToledo-Morrell, L., 2001. MRI-derived entorhinal and hippocampal atrophy in incipient and very mild Alzheimer's disease. Neurobiol. Aging 22, 747–754.

Du, A.T., Schuff, N., Amend, D., Laakso, M.P., Hsu, Y.Y., Jagust, W.J., Yaffe, K., Kramer, J.H., Reed, B., Norman, D., Chui, H.C., Weiner, M.W., 2001. Magnetic resonance imaging of the entorhinal cortex and hippocampus in mild cognitive impairment and Alzheimer's disease. J. Neurol. Neurosurg. Psychiatry 71, 441–447.

Du, A.T., Schuff, N., Chao, L.L., Kornak, J., Jagust, W.J., Kramer, J.H., Reed, B.R., Miller, B.L., Norman, D., Chui, H.C., Weiner, M.W., 2006. Age effects on atrophy rates of entorhinal cortex and hippocampus. Neurobiol. Aging 27, 733–740.

Du, A.T., Schuff, N., Kramer, J.H., Rosen, H.J., Gorno-Tempini, M.L., Rankin, K., Miller, B.L., Weiner, M.W., 2007. Different regional patterns of cortical thinning in Alzheimer's disease and frontotemporal dementia. Brain 130, 1159–1166.

Erten-Lyons, D., Howieson, D., Moore, M.M., Quinn, J., Sexton, G., Silbert, L., Kaye, J., 2006. Brain volume loss in MCI predicts dementia. Neurology 66, 233–235.

Evans, M.C., Barnes, J., Nielsen, C., Kim, L.G., Clegg, S.L., Blair, M., Leung, K.K., Douiri, A., Boyes, R.G., Ourselin, S., Fox, N.C., 2009. Volume changes in Alzheimer's disease and mild cognitive impairment: cognitive associations. Eur. Radiol. 20, 674–682.

Fan, Y., Batmanghelich, N., Clark, C.M., Davatzikos, C., 2008. Spatial patterns of brain atrophy in MCI patients, identified via high-dimensional pattern classification, predict subsequent cognitive decline. Neuroimage 39, 1731–1743.

Farrer, L.A., Cupples, L.A., Haines, J.L., Hyman, B., Kukull, W.A., Mayeux, R., Myers, R.H., Pericak-Vance, M.A., Risch, N., van Duijn, C.M., 1997. Effects of age, sex, and ethnicity on the association between apolipoprotein E genotype and Alzheimer disease. A meta-analysis. APOE and Alzheimer Disease Meta Analysis Consortium. JAMA 278, 1349–1356.

Fennema-Notestine, C., Hagler, D.J., Jr, McEvoy, L.K., Fleisher, A.S., Wu, E.H., Karow, D.S., Dale, A.M., 2009. Structural MRI biomarkers for preclinical and mild Alzheimer's disease. Hum. Brain Mapp. 30, 3238–3253.

Ferri, C.P., Prince, M., Brayne, C., Brodaty, H., Fratiglioni, L., Ganguli, M., Hall, K., Hasegawa, K., Hendrie, H., Huang, Y., Jorm, A., Mathers, C., Menezes, P.R., Rimmer, E., Scazufca, M., 2005. Global prevalence of dementia: a Delphi consensus study. Lancet 366, 2112–2117.

Fischl, B., Dale, A.M., 2000a. Measuring the thickness of the human cerebral cortex from magnetic resonance images. Proc. Natl. Acad. Sci. U. S. A. 97, 11050–11055.

Fischl, B., Dale, A.M., 2000b. Measuring the thickness of the human cerebral cortex from magnetic resonance images. Proc. Natl. Acad. Sci. U. S. A. 97, 11050–11055.

Fischl, B., Salat, D., Busa, E., Albert, M., Dieterich, M., Haselgrove, C., van der Kouwe, A., Killiany, R., Kennedy, D., Klaveness, S., Montillo, A., Makris, N., Rosen, B., Dale, A., 2002. Whole brain segmentation: automated labeling of neuroanatomical structures in the human brain. Neuron 33, 341–355.

Fischl, B., Sereno, M., Dale, A., 1999. Cortical surface-based analysis. II: Inflation, flattening, and a surface-based coordinate system. Neuroimage 9, 195–207.

Fjell, A.M., Walhovd, K.B., Fennema-Notestine, C., McEvoy, L.K., Hagler, D.J., Holland, D., Blennow, K., Brewer, J.B., Dale, A.M., 2010a. Brain Atrophy in Healthy Aging Is Related to CSF Levels of A{beta} 1–42. Cereb. Cortex, doi:10.1093/cercor/bhp279.

Fjell, A.M., Walhovd, K.B., Fennema-Notestine, C., McEvoy, L.K., Hagler, D.J., Holland, D., Brewer, J., Dale, A., ADNI, 2010b. CSF Biomarkers in Prediction of Cerebral and Clinical Change in Mild Cognitive Impairment and Alzheimer's Disease. J. Neurosci. 30, 2088–2101.

Fleisher, A., Grundman, M., Jack, C.R., Jr, Petersen, R.C., Taylor, C., Kim, H.T., Schiller, D.H., Bagwell, V., Sencakova, D., Weiner, M.F., deCarli, C., deKosky, S.T., van Dyck, C.H., Thal, L.J., 2005. Sex, apolipoprotein E epsilon 4 status, and hippocampal volume in mild cognitive impairment. Arch. Neurol. 62, 953–957.

Fleisher, A.S., Sun, S., Taylor, C., Ward, C.P., Gamst, A.C., Petersen, R.C., Jack, C.R., Jr, Aisen, P.S., Thal, L.J., 2008. Volumetric MRI vs clinical predictors of Alzheimer disease in mild cognitive impairment. Neurology 70, 191–199.

Fox, N.C., Freeborough, P.A., 1997. Brain atrophy progression measured from registered serial MRI: validation and application to Alzheimer's disease. J. Magn. Reson. Imaging 7, 1069–1075.

Frisoni, G.B., Fox, N.C., Jack, C.R., Jr, Scheltens, P., Thompson, P.M., 2010. The clinical use of structural MRI in Alzheimer disease. Nat. Rev. Neurol. 6, 67–77.

Frisoni, G.B., Testa, C., Zorzan, A., Sabattoli, F., Beltramello, A., Soininen, H., Laakso, M.P., 2002. Detection of grey matter loss in mild Alzheimer's disease with voxel based morphometry. J. Neurol. Neurosurg. Psychiatry 73, 657–664.

Gatz, M., Reynolds, C.A., Fratiglioni, L., Johansson, B., Mortimer, J.A., Berg, S., Fiske, A., Pedersen, N.L., 2006. Role of genes and environments for explaining Alzheimer disease. Arch. Gen. Psychiatry 63, 168–174.

Good, C.D., Johnsrude, I.S., Ashburner, J., Henson, R.N., Friston, K.J., Frackowiak, R.S., 2001. A voxel-based morphometric study of ageing in 465 normal adult human brains. Neuroimage 14, 21–36.

Hamalainen, A., Grau-Olivares, M., Tervo, S., Niskanen, E., Pennanen, C., Huuskonen, J., Kivipelto, M., Hanninen, T., Tapiola, M., Vanhanen, M., Hallikainen, M., Helkala, E.L., Nissinen, A., Vanninen, R.L., Soininen, H., 2008. Apolipoprotein E epsilon4 allele is associated with increased atrophy in progressive mild cognitive impairment: a voxel-based morphometric study. Neurodegeneration 5, 186–189.

Ho, A.J., Hua, X., Lee, S., Leow, A.D., Yanovsky, I., Gutman, B., Dinov, I.D., Lepore, N., Stein, J.L., Toga, A.W., Jack, C.R., Jr., Bernstein, M.A., Reiman, E.M., Harvey, D.J., Kornak, J., Schuff, N., Alexander, G.E., Weiner, M.W., Thompson, P.M., 2009. Comparing 3 T and 1.5 T MRI for tracking Alzheimer's disease progression with tensor-based morphometry. Hum. Brain Mapp 31, 499–514.

Holland, D., Brewer, J.B., Hagler, D.J., Fenema-Notestine, C., Dale, A.M., Weiner, M., Thal, L., Petersen, R., Jack, C.R., Jr, Jagust, W., Trojanowki, J., Toga, A.W., Beckett, L., ADNI, 2009. Subregional neuroanatomical change as a biomarker for Alzheimer's disease. Proc. Natl. Acad. Sci. U. S. A. 106, 20954–20959.

Hua, X., Lee, S., Yanovsky, I., Leow, A.D., Chou, Y.Y., Ho, A.J., Gutman, B., Toga, A.W., Jack, C.R., Jr, Bernstein, M.A., Reiman, E.M., Harvey, D.J., Kornak, J., Schuff, N., Alexander, G.E., Weiner, M.W., Thomp-

son, P.M., 2009. Optimizing power to track brain degeneration in Alzheimer's disease and mild cognitive impairment with tensor-based morphometry: an ADNI study of 515 subjects. Neuroimage 48, 668–681.

Jack, C.R., Jr., Bernstein, M.A., Fox, N.C., Thompson, P., Alexander, G., Harvey, D., Borowski, B., Britson, P.J., L. Whitwell, J., Ward, C., Dale, A.M., Felmlee, J.P., Gunter, J.L., Hill, D.L., Killiany, R., Schuff, N., Fox-Bosetti, S., Lin, C., Studholme, C., deCarli, C.S., Krueger, G., Ward, H.A., Metzger, G.J., Scott, K.T., Mallozzi, R., Blezek, D., Levy, J., Debbins, J.P., Fleisher, A.S., Albert, M., Green, R., Bartzokis, G., Glover, G., Mugler, J., Weiner, M.W., 2008a. The Alzheimer's Disease Neuroimaging Initiative (ADNI): MRI methods. J. Magn. Reson. Imaging 27, 685–691.

Jack, C.R., Jr, Lowe, V.J., Senjem, M.L., Weigand, S.D., Kemp, B.J., Shiung, M.M., Knopman, D.S., Boeve, B.F., Klunk, W.E., Mathis, C.A., Petersen, R.C., 2008b. 11C PiB and structural MRI provide complementary information in imaging of Alzheimer's disease and amnestic mild cognitive impairment. Brain 131, 665–680.

Jack, C.R., Jr, Lowe, V.J., Weigand, S.D., Wiste, H.J., Senjem, M.L., Knopman, D.S., Shiung, M.M., Gunter, J.L., Boeve, B.F., Kemp, B.J., Weiner, M., Petersen, R.C., 2009. Serial PIB and MRI in normal, mild cognitive impairment and Alzheimer's disease: implications for sequence of pathological events in Alzheimer's disease. Brain 132, 1355–1365.

Jack, C.R., Jr, Petersen, R.C., Grundman, M., Jin, S., Gamst, A., Ward, C.P., Sencakova, D., Doody, R.S., Thal, L.J., 2008c. Longitudinal MRI findings from the vitamin E and donepezil treatment study for MCI. Neurobiol. Aging 29, 1285–1295.

Jack, C.R., Jr, Petersen, R.C., O'Brien, P.C., Tangalos, E.G., 1992. MR-based hippocampal volumetry in the diagnosis of Alzheimer's disease. Neurology 42, 183–188.

Jack, C.R., Jr, Petersen, R.C., Xu, Y., O'Brien, P.C., Smith, G.E., Ivnik, R.J., Boeve, B.F., Tangalos, E.G., Kokmen, E., 2000. Rates of hippocampal atrophy correlate with change in clinical status in aging and AD. Neurology 55, 484–489.

Jack, C.R., Jr, Petersen, R.C., Xu, Y.C., O'Brien, P.C., Smith, G.E., Ivnik, R.J., Boeve, B.F., Waring, S.C., Tangalos, E.G., Kokmen, E., 1999. Prediction of AD with MRI-based hippocampal volume in mild cognitive impairment. Neurology 52, 1397–1403.

Jack, C.R., Jr, Shiung, M.M., Gunter, J.L., O'Brien, P.C., Weigand, S.D., Knopman, D.S., Boeve, B.F., Ivnik, R.J., Smith, G.E., Cha, R.H., Tangalos, E.G., Petersen, R.C., 2004. Comparison of different MRI brain atrophy rate measures with clinical disease progression in AD. Neurology 62, 591–600.

Jack, C.R., Jr, Shiung, M.M., Weigand, S.D., O'Brien, P.C., Gunter, J.L., Boeve, B.F., Knopman, D.S., Smith, G.E., Ivnik, R.J., Tangalos, E.G., Petersen, R.C., 2005. Brain atrophy rates predict subsequent clinical conversion in normal elderly and amnestic MCI. Neurology 65, 1227–1231.

Jack, C.R., Jr, Weigand, S.D., Shiung, M.M., Przybelski, S.A., O'Brien, P.C., Gunter, J.L., Knopman, D.S., Boeve, B.F., Smith, G.E., Petersen, R.C., 2008d. Atrophy rates accelerate in amnestic mild cognitive impairment. Neurology 70, 1740–1752.

Karas, G.B., Burton, E.J., Rombouts, S.A., van Schijndel, R.A., O'Brien, J.T., Scheltens, P., McKeith, I.G., Williams, D., Ballard, C., Barkhof, F., 2003. A comprehensive study of gray matter loss in patients with Alzheimer's disease using optimized voxel-based morphometry. Neuroimage 18, 895–907.

Killiany, R.J., Hyman, B.T., Gomez-Isla, T., Moss, M.B., Kikinis, R., Jolesz, F., Tanzi, R., Jones, K., Albert, M.S., 2002. MRI measures of entorhinal cortex vs hippocampus in preclinical. Adv. Neurol. 58, 1188–1196.

Kinkingnehun, S., Sarazin, M., Lehericy, S., Guichart-Gomez, E., Hergueta, T., Dubois, B., 2008. VBM anticipates the rate of progression of Alzheimer disease: a 3-year longitudinal study. Neurology 70, 2201–2211.

Leow, A.D., Yanovsky, I., Parikshak, N., Hua, X., Lee, S., Toga, A.W., Jack, C.R., Jr., Bernstein, M.A., Britson, P.J., Gunter, J.L., Ward, C.P., Borowski, B., Shaw, L.M., Trojanowski, J.Q., Fleisher, A.S., Harvey, D., Kornak, J., Schuff, N., Alexander, G.E., Weiner, M.W., Thompson, P.M., 2009. Alzheimer's Disease Neuroimaging Initiative: A one-year follow up study using Tensor-Based Morphometry correlating degenerative rates, biomarkers and cognition. Neuroimage 45, 645–55.

McDonald, C.R., McEvoy, L.K., Gharapetian, L., Fennema-Notestine, C., Hagler, D.J., Jr, Holland, D., Koyama, A., Brewer, J.B., Dale, A.M., 2009. Regional rates of neocortical atrophy from normal aging to early Alzheimer disease. Neurology 73, 457–465.

McEvoy, L.K., Fennema-Notestine, C., Roddey, J.C., Hagler, D.J., Jr, Holland, D., Karow, D.S., Pung, C.J., Brewer, J.B., Dale, A.M., 2009. Alzheimer disease: quantitative structural neuroimaging for detection and prediction of clinical and structural changes in mild cognitive impairment. Radiology 251, 195–205.

McHugh, T., Saykin, A., Wishart, H., Flashman, L., Cleavinger, H., Rabin, L., Mamourian, A., Shen, L., 2007. Hippocampal volume and shape analysis in an older adult population. Clin. Neuropsychol. 21, 130–145.

Mechelli, A., Price, C.J., Friston, K.J., Ashburner, J., 2005. Voxel based morphometry of the human brain: methods and applications. Current Medical Imaging Reviews 1, 1–9.

Misra, C., Fan, Y., Davatzikos, C., 2009. Baseline and longitudinal patterns of brain atrophy in MCI patients, and their use in prediction of short-term conversion to AD: results from ADNI. Neuroimage 44, 1415–1422.

Mori, E., Lee, K., Yasuda, M., Hashimoto, M., Kazui, H., Hirono, N., Matsui, M., 2002. Accelerated hippocampal atrophy in Alzheimer's disease with apolipoprotein E epsilon4 allele. Ann. Neurol. 51, 209–214.

Morra, J.H., Tu, Z., Apostolova, L.G., Green, A.E., Avedissian, C., Madsen, S.K., Parikshak, N., Toga, A.W., Jack, C.R., Jr, Schuff, N., Weiner, M.W., Thompson, P.M., 2009. Automated mapping of hippocampal atrophy in 1-year repeat MRI data from 490 subjects with Alzheimer's disease, mild cognitive impairment, and elderly controls. Neuroimage 45 Suppl, S3–S15.

Mueller, S.G., Weiner, M.W., Thal, L.J., Petersen, R.C., Jack, C., Jagust, W., Trojanowski, J.Q., Toga, A.W., Beckett, L., 2005a. The Alzheimer's disease neuroimaging initiative. Neuroimaging Clin. N Am. 15, 869–877, xi–xii.

Mueller, S.G., Weiner, M.W., Thal, L.J., Petersen, R.C., Jack, C.R., Jagust, W., Trojanowski, J.Q., Toga, A.W., Beckett, L., 2005b. Ways toward an early diagnosis in Alzheimer's disease: The Alzheimer's Disease Neuroimaging Initiative (ADNI). Alzheimers Dement. 1, 55–66.

Mungas, D., Harvey, D., Reed, B.R., Jagust, W.J., deCarli, C., Beckett, L., Mack, W.J., Kramer, J.H., Weiner, M.W., Schuff, N., Chui, H.C., 2005. Longitudinal volumetric MRI change and rate of cognitive decline. Neurology 65, 565–571.

Nestor, S.M., Rupsingh, R., Borrie, M., Smith, M., Accomazzi, V., Wells, J.L., Fogarty, J., Bartha, R., 2008. Ventricular enlargement as a possible measure of Alzheimer's disease progression validated using the Alzheimer's disease neuroimaging initiative database. Brain 131, 2443–2454.

Pennanen, C., Kivipelto, M., Tuomainen, S., Hartikainen, P., Hanninen, T., Laakso, M.P., Hallikainen, M., Vanhanen, M., Nissinen, A., Helkala, E.L., Vainio, P., Vanninen, R., Partanen, K., Soininen, H., 2004. Hippocampus and entorhinal cortex in mild cognitive impairment and early AD. Neurobiol. Aging 25, 303–310.

Pennanen, C., Testa, C., Laakso, M.P., Hallikainen, M., Helkala, E.L., Hanninen, T., Kivipelto, M., Kononen, M., Nissinen, A., Tervo, S., Vanhanen, M., Vanninen, R., Frisoni, G.B., Soininen, H., 2005. A voxel based morphometry study on mild cognitive impairment. J. Neurol. Neurosurg. Psychiatry 76, 11–14.

Petersen, R.C., 2000. Mild cognitive impairment: transition between aging and Alzheimer's disease. Neurologia 15, 93–101.

Petersen, R.C., Aisen, P.S., Beckett, L.A., Donohue, M.C., Gamst, A.C., Harvey, D.J., Jack, C.R., Jr., Jagust, W.J., Shaw, L.M., Toga, A.W., Trojanowski, J.Q., Weiner, M.W., 2010a. Alzheimer's Disease Neuroimaging Initiative (ADNI): Clinical characterization. Neurology 74, 201–209.

Petersen, R.C., Doody, R., Kurz, A., Mohs, R.C., Morris, J.C., Rabins, P.V., Ritchie, K., Rossor, M., Thal, L., Winblad, B., 2001. Current concepts in mild cognitive impairment. Arch. Neurol. 58, 1985–1992.

Petersen, R.C., Negash, S., 2008. Mild cognitive impairment: an overview. CNS Spectr 13, 45–53.

Petersen, R.C., Smith, G.E., Waring, S.C., Ivnik, R.J., Tangalos, E.G., Kokmen, E., 1999. Mild cognitive impairment: clinical characterization and outcome. Arch. Neurol. 56, 303–308.

Querbes, O., Aubry, F., Pariente, J., Lotterie, J.A., Demonet, J.F., Duret, V., Puel, M., Berry, I., Fort, J.C., Celsis, P., 2009. Early diagnosis of Alzheimer's disease using cortical thickness: impact of cognitive reserve. Brain 132, 2036–2047.

Risacher, S.L., Saykin, A.J., in press. Neuroimaging of Alzheimer's Disease, Mild Cognitive Impairment and Other Dementias, in: Sweet, L.H., Cohen, R.A., (Eds.), Brain Imaging in Behavioral Medicine and Neuropsychology. Springer, New York.

Risacher, S.L., Saykin, A.J., West, J.D., Shen, L., Firpi, H.A., McDonald, B.C., 2009. Baseline MRI predictors of conversion from MCI to probable AD in the ADNI cohort. Curr. Alzheimer Res. 6, 347–361.

Rosner, B., 1990. Fundamentals of Biostatistics. PWS-Kent Publishing Company, Boston.

Saykin, A., Wishart, H., Rabin, L., Santulli, R., Flashman, L., West, J., McHugh, T., Mamourian, A., 2006. Older adults with cognitive complaints show brain atrophy similar to that of amnestic MCI. Neurology 67, 834–842.

Saykin, A.J., Shen, L., Foroud, T., Potkin, S.G., Swaminathan, S., Kim, S., Risacher, S.L., Nho, K., Huentelman, M.J., Craig, D.W., Thompson, P.M., Stein, J.L., Moore, J.H., Farrer, L.A., Green, R.C., Bertram, L., Jack, C.R., Weiner, M.W., ADNI, 2010. Alzheimer's Disease Neuroimaging Initiative biomarkers as quantitative phenotypes: genetics core aims, progress, and plans. Alzheimers Dement. 6, 1–9.

Saykin, A.J., Shen, L., Risacher, S.L., Kim, S., Nho, K., West, J.D., Foroud, T., ADNI, 2009. Genetic predictors of 12 month change in MRI hippocampal volume in the Alzheimer's Disease Neuroimaging Initiative cohort: Analysis of leading candidates from the AlzGene database. Alzheimers Dement 5(4), P3.

Schuff, N., Woerner, N., Boreta, L., Kornfield, T., Shaw, L.M., Trojanowski, J.Q., Thompson, P.M., Jack, C.R., Jr, Weiner, M.W., 2009. MRI of hippocampal volume loss in early Alzheimer's disease in relation to ApoE genotype and biomarkers. Brain 132, 1067–1077.

Shen, L., Saykin, A.J., Kim, S., Firpi, H., West, J.D., Risacher, S.L., McDonald, B.C., McHugh, T.L., Wishart, H.A., Flashman, L.A., 2010. Comparison of manual and automated determination of hippocampal volumes in MCI and older adults with cognitive complaints. Brain Imaging Behav., doi:10.1007/s11682-010-9088-x.

Sluimer, J.D., Vrenken, H., Blankenstein, M.A., Fox, N.C., Scheltens, P., Barkhof, F., van der Flier, W.M., 2008. Whole-brain atrophy rate in Alzheimer disease: identifying fast progressors. Neurology 70, 1836–1841.

Stoub, T.R., Rogalski, E.J., Leurgans, S., Bennett, D.A., Detoledo-Morrell, L., 2008. Rate of entorhinal and hippocampal atrophy in incipient and mild AD: relation to memory function. Neurobiol. Aging 31(7), 1089–98.

Thompson, P.M., Hayashi, K.M., De Zubicaray, G.I., Janke, A.L., Rose, S.E., Semple, J., Hong, M.S., Herman, D.H., Gravano, D., Doddrell, D.M., Toga, A.W., 2004. Mapping hippocampal and ventricular change in Alzheimer disease. Neuroimage 22, 1754–1766.

Trivedi, M.A., Wichmann, A.K., Torgerson, B.M., Ward, M.A., Schmitz, T.W., Ries, M.L., Koscik, R.L., Asthana, S., Johnson, S.C., 2006. Structural MRI discriminates individuals with Mild Cognitive Impairment from age-matched controls: A combined neuropsychological and voxel based morphometry study. Alzheimers Dement. 2, 296–302.

Vemuri, P., Wiste, H.J., Weigand, S.D., Shaw, L.M., Trojanowski, J.Q., Weiner, M.W., Knopman, D.S., Petersen, R.C., Jack, C.R., Jr, 2009. MRI and CSF biomarkers in normal, MCI, and AD subjects: diagnostic discrimination and cognitive correlations. Neurology 73, 287–293.

Visser, P.J., Verhey, F.R., Hofman, P.A., Scheltens, P., Jolles, J., 2002. Medial temporal lobe atrophy predicts Alzheimer's disease in patients with minor cognitive impairment. J. Neurol. Neurosurg. Psychiatry 72, 491–497.

Walhovd, K.B., Fjell, A.M., Dale, A.M., McEvoy, L.K., Brewer, J., Karow, D.S., Salmon, D.P., and ADNI, 2010. Multi-modal imaging predicts memory performance in normal aging and cognitive decline. Neurobiology of Aging 31(7), 1107–1121.

Wang, P.N., Lirng, J.F., Lin, K.N., Chang, F.C., Liu, H.C., 2006. Prediction of Alzheimer's disease in mild cognitive impairment: a prospective study in Taiwan. Neurobiol. Aging 27, 1797–1806.

Wang, P.N., Liu, H.C., Lirng, J.F., Lin, K.N., Wu, Z.A., 2009. Accelerated hippocampal atrophy rates in stable and progressive amnestic mild cognitive impairment. Psychiatry Res. 171, 221–231.

Whitwell, J.L., Jack, C.R., Jr, Pankratz, V.S., Parisi, J.E., Knopman, D.S., Boeve, B.F., Petersen, R.C., Dickson, D.W., Josephs, K.A., 2008a. Rates of brain atrophy over time in autopsy-proven frontotemporal dementia and Alzheimer disease. Neuroimage 39, 1034–1040.

Whitwell, J.L., Shiung, M.M., Przybelski, S.A., Weigand, S.D., Knopman, D.S., Boeve, B.F., Petersen, R.C., Jack, C.R., Jr, 2008b. MRI patterns of atrophy associated with progression to AD in amnestic mild cognitive impairment. Neurology 70, 512–520.

Wimo, A., Winblad, B., Aguero-Torres, H., von Strauss, E., 2003. The magnitude of dementia occurrence in the world. Alzheimer Dis. Assoc. Disord. 17, 63–67.

Xu, Y., Jack, C.R., Jr., O'Brien, P.C., Kokmen, E., Smith, G.E., Ivnik, R.J., Boeve, B.F., Tangalos, R.G., Petersen, R.C., 2000. Usefulness of MRI measures of entorhinal cortex versus hippocampus in AD. Neurology 54, 1760–1767.